

CO₂, N₂ and Ar Adsorption on Zeolites

By

Aslı ERTAN

A Dissertation Submitted to the
Graduate School in Partial Fulfillment of the
Requirements for the Degree of

MASTER OF SCIENCE

Department: Chemical Engineering

Major: Chemical Engineering

**İzmir Institute of Technology
İzmir, Turkey**

February, 2004

We approve the thesis of **Aslı ERTAN**

Date of Signature

.....

10.02.2004

Asst. Prof. S. Fehime ÖZKAN

Supervisor

Department of Chemical Engineering

.....

10.02.2004

Prof. Dr. A. Semra ÜLKÜ

Co-Supervisor

Department of Chemical Engineering

.....

10.02.2004

Prof. Dr. Devrim BALKÖSE

Department of Chemical Engineering

.....

10.02.2004

Prof. Dr. Gönül GÜNDÜZ

Department of Chemical Engineering

.....

10.02.2004

Asst. Prof. Aysun SOFUOĞLU

Department of Chemical Engineering

.....

10.02.2004

Prof. Dr. Devrim BALKÖSE

Head of Department

ACKNOWLEDGEMENTS

I would like to express my intimate gratitude to my advisor, Asst. Prof. Fehime Özkan, for her guidance and support throughout this project. I am also grateful to Prof. Dr. Semra Ülkü and Prof. Dr. Devrim Balköse for their valuable suggestions. I also would like to give my special thanks to Asst. Prof. Erol Şeker for his valuable recommendations during the study.

I would like to thank all of the experts in the Chemical Engineering Department of İzmir Institute of Technology, laboratory technicians and especially to the experts Nesrin Tatlıdil, Burcu Alp and Özlem Çağlar for their contributions to the volumetric and calorimetric studies presented in this study.

I would like to acknowledge deeply to my roommates, Öniz Birsoy, Emre Kuduğ, Belgin Tunçel and also Hilal Güleç for their friendships, supports and encouragements.

My special thanks also go to my family and finally to my fiancé Özge Can for their support, patience and understanding.

ABSTRACT

In this study, CO₂ and N₂ adsorption on synthetic zeolites namely, 5A and 13X, and acid treated natural zeolites was investigated by using volumetric adsorption device, ASAP 2010. The natural zeolites and its acid treated forms with HCl (1M, 3M and 5M), HNO₃ (2 M), and H₃PO₄ (1.1 M) solutions at 60 °C for 6 or 3 hours were used as adsorbent. The effect of the acid treatment and temperature on the adsorption properties of the zeolites for the CO₂ and N₂ gases at 5 and 25 °C was studied. Langmuir, Sips, Vrial and Dubinin-Astakhov model equations were applied to the adsorption data in order to determine the affinity and the heterogeneity of the adsorbents.

Calorimetric properties of the zeolites were also studied using CO₂, N₂ and Ar gases through a Tian-Calvet calorimeter, Setaram C80 at 25 °C. Isotheric heat of adsorption of the gases adsorbed on the adsorbents under investigation was determined at 5 °C and 25 °C using Clasius- Clapeyron equation. These results were compared with the heat of adsorptions obtained from the calorimetric studies directly.

The zeolite treated with 1.1 M H₃PO₄, P1 has the highest adsorption capacity (2.24 mmol/g and 0.67 mmol/g) for CO₂ and N₂ while the natural zeolite has only 2.08 mmol/g and 0.51 mmol/g respectively at 5 °C. Synthetic zeolites 13X and 5A have higher CO₂ (6.82 mmol/g and 5.46 mmol/g respectively) and N₂ adsorption capacities (0.31mmol/g and 0.91 mmol/g respectively) than natural zeolites at 5 °C. Langmuir b parameter called the affinity constant decreased as adsorption temperature increased for CO₂ and N₂ adsorption. The Sips model t parameter characterizing the system heterogeneity is higher for CO₂ adsorption than N₂ adsorption and decreases with increasing temperature. This indicates that the CO₂ molecules give more specific interactions than N₂ molecules. The pure component selectivities of CO₂ over N₂ calculated from Langmuir equation, are the highest for NCW zeolite as 408 at 25 °C. This value follows by P1 zeolite which is 151 at the same temperature.

The highest differential heat of adsorption value (80.29 kJ/mol) at zero coverage for CO₂ also belongs to P1 sample. The heterogeneity parameters of the model equations applied also indicated that P1 sample is more heterogeneous when compared to other acid treated natural zeolites. Finally as expected, for both N₂ and CO₂ as temperature increased from 5 to 25 °C, the adsorbed amounts decreased when fresh samples were used at each run in the experiments. The temperature difference had a greater effect on N₂ adsorption rather than CO₂.

ÖZ

Bu çalışmada 5A ve 13X sentetik zeolitleri ile doğal zeolitlerin asit ile işlem görmüş formlarında CO₂ ve N₂ adsorpsiyonları volumetric system kullanılarak (ASAP 2010) çalışılmıştır. Doğal zeolitler HCl (1M, 3M and 5M), HNO₃ (2 M), ve H₃PO₄ (1.1 M) çözeltileriyle 60 °C'de 3 veya 6 saat işleme tabi tutulmuştur. Asit işlemlerinin doğal zeolitlerin CO₂ ve N₂ adsorpsiyonlarına 5 ve 25 °C'deki etkisi incelenmiştir. Elde edilen adsorpsiyon verilerine birçok model denklem uygulanmıştır. Bu şekilde adsorbentlerin heterojeniteleriyle ilgili bilgi edinilip sonuçlar yapay zeolitlerle karşılaştırılmıştır. Ayrıca sıcaklığın CO₂ ve N₂ adsorpsiyonlarına olan etkisi çalışılmıştır.

Öte yandan, mikrokalorimetre Setaram C80 cihazı kullanılarak zeolitlerin CO₂, N₂ ve Ar gazları kullanılarak kalorimetrik özellikleri incelenmiştir. Clasius-Clapeyron denklemi kullanılarak gazların isosterik adsorpsiyon ısıları teorik olarak hesaplanıp sonuçlar deneysel olarak elde edilenlerle karşılaştırılmıştır.

Adsorpsiyon çalışmaları, doğal zeolitler arasında 5 °C'de, CO₂ ve N₂ için en yüksek adsorplama kapasitesine sahip adsorbentin 1.1 M H₃PO₄ çözeltisiyle işlem görmüş P1 (2.24 mmol/g ve 0.67 mmol/g) örneği olduğunu, doğal zeolitin ise bu gazlar için adsorplama kapasitelerinin sırasıyla 2.08 mmol/g and 0.51 mmol/g olduğunu göstermiştir. 13X ve 5A sentetik zeolitleri 5 °C'de doğal zeolitlere göre daha yüksek CO₂ (sırasıyla 6.82 mmol/g ve 5.46 mmol/g) ve N₂ (0.31mmol/g and 0.91 mmol/g) adsorplama kapasitesine sahiptir. Langmuir b parametresi N₂ adsorpsiyonunda sıcaklık arttıkça düşmüştür. CO₂ adsorpsiyonunda ise sıcaklık ile artmıştır. Sistem heterojenitesini karakterize eden t parametresi CO₂ adsorpsiyonunda daha yüksektir ve sıcaklık arttıkça düşmüştür. Bu durum CO₂ molekülünün N₂'ye göre daha çok spesifik etkileşim verdiğini göstermektedir. Langmuir denkleminde hesaplanan CO₂'in N₂'ye göre seçiciliği 25 °C'de 408 olup NCW örneğinde en yüksektir. Aynı sıcaklıkta P1 örneği için bu değer 151'dir.

CO₂ için maksimum diferansiyel adsorpsiyon ısı 80.29 kJ/mol ile P1örneğine aittir. Uygulanan model denklemlerin heterojenite parametreleri de P1'in diğer örneklere göre daha heterojen olduğunu göstermiştir. Bütün bunlar P1 örneğinin gazlarla oluşturduğu spesifik etkileşimlerin diğer örneklere göre daha fazla olduğunu göstermiştir. Son olarak, beklenildiği üzere adsorpsiyon sıcaklığı arttıkça her bir deneyde yeni örnek kullanıldığında adsorplanan miktar düşmüştür. Sıcaklık farkının CO₂'e göre N₂ adsorpsiyona etkisinin daha fazla olduğu görülmüştür.

TABLE OF CONTENTS

	Page
LIST OF FIGURES.....	xi
LIST OF TABLES.....	xiii
CHAPTER 1. INTRODUCTION.....	1
CHAPTER 2. ZEOLITES.....	3
2.1. Definition.....	3
2.2. Structure.....	4
2.3. Clinoptilolite-rich Natural Zeolite Tuff.....	5
2.4. Synthetic Zeolites.....	9
2.5. Uses and Applications	10
CHAPTER 3. ADSORPTION.....	12
3.1. Definition.....	12
3.2. Adsorbents.....	12
3.3. Properties of the Adsorbate Gases Used in this Study.....	14
3.3.1. Carbondioxide.....	14
3.3.2. Nitrogen.....	14
3.3.3. Argon.....	15
3.4. Pure Gas Adsorption Isotherms.....	15
3.4.1. Langmuir Model.....	16
3.4.2. Dubinin Model.....	17
3.4.3. Emprical Isotherm Equations.....	19
3.4.4. Henry's Law.....	20
CHAPTER 4. GAS SEPARATION.....	22
4.1. Factors Affecting Separation.....	22

4.1.1. Adsorbent-adsorbate Interactions.....	22
4.1.2. Surface Structure of the Adsorbent.....	23
4.1.3. Heat of Adsorption.....	25
4.2. Selectivity.....	26
4.3. Selectivity Control.....	27
4.4. Ideal Adsorbed Solution Theory (IAST).....	28
4.4.1. Solution Strategy	30
 CHAPTER 5. EXPERIMENTAL.....	 33
5.1 Materials.....	33
5.2 Methods.....	36
5.2.1. Adsorption Studies.....	36
5.2.2. Calorimetric Studies.....	37
 CHAPTER 6. RESULTS AND DISCUSSION.....	 40
6.1. Adsorption Studies.....	40
6.1.1. Adsorption Isotherms.....	40
6.1.2. Adsorption Capacities of the Zeolites for CO ₂ and N ₂ Adsorption	44
6.1.3. Model Equations.....	47
6.1.4. Evaluation of the Energy Distributions.....	55
6.2. Calorimetric Studies.....	60
6.2.1. Calorimetric Peaks of CO ₂ , N ₂ and Ar on Zeolites.....	61
6.3 Determination of the Isothermic Heat of Adsorption.....	70
 CONCLUSION.....	 74
 REFERENCES.....	 76
 APPENDIX.....	 79

LIST OF FIGURES		Page
Figure 2.1	Secondary Building Units (SBU's) in zeolites. The corner of the polyhedra represent tetrahedral atoms.....	4
Figure 2.2	The c-axis projection of the structure of clinoptilolite, showing the cation positions in the structure.....	6
Figure 2.3	Schematic diagram of clinoptilolite structure	8
Figure 2.4	Center occupied by Si ⁺⁴ or Al ⁺³ atom with four O atoms at the corners.....	8
Figure 2.5	Tetrahedron-primary building unit.....	8
Figure 2.6	Structure of Zeolite A.....	9
Figure 2.7	Structure of X and Y synthetic zeolites	10
Figure 3.1.	The six main types of gas physisorption isotherms.....	15
Figure 5.1	X-ray diffraction patterns of the washed natural zeolite (NCW)..	35
Figure 5.2	SEM Micrographs of the zeolites.....	35
Figure 5.3	Photograph of the Microcalorimetry System	39
Figure 6.1	CO ₂ Adsorption Isotherms on the used and fresh Adsorbents at 5 °C (●); 25 °C (○).....	42
Figure 6.2	N ₂ Adsorption Isotherms on the zeolites at 5 °C (●); 25 °C (○).....	43
Figure 6.3	CO ₂ Adsorption Isotherms on the zeolites at 5 °C (●); 25 °C (○). Points: experimental data, lines: Langmuir Model, dashed lines: Sips Model.....	51
Figure 6.4	N ₂ Adsorption Isotherms on the zeolites at 5 °C (●); 25 °C (○). Points: experimental data, lines: Langmuir Model, dashed lines: Sips Model.....	52
Figure 6.5	Change of Selectivity Ratios with Si/Al at 25°C.....	54
Figure 6.6	Adsorption Potential Distributions for CO ₂ Adsorption at 5 °C (●); 25 °C (○).....	56
Figure 6.7	Adsorption Potential Distributions for N ₂ Adsorption at 5 °C (●); 25 °C (○).....	57
Figure 6.8	Adsorption Potential Distributions for (A) CO ₂ , (B) N ₂ Adsorptions at 25 °C.....	58
Figure 6.9	Characterisitic Energies of the Zeolites for N ₂ at 25 ⁰ C.....	59
Figure 6.10	Characterisitic Energies of the Zeolites for N ₂ at 5 ⁰ C.....	59

Figure 6.11	A set of calorimetric peaks obtained for CO ₂ , N ₂ and Ar adsorptions on the zeolites (C1-6h: 300 mbar dose intervals, others 50 and 300 mbar dose intervals.....	62
Figure 6.12	Differential Heat of Adsorption of CO ₂ on zeolites	63
Figure 6.13	Differential Heat of Adsorption of N ₂ on Zeolites.....	66
Figure 6.14	Differential Heat of Adsorption of Ar on Zeolites.....	68

LIST OF TABLES

Table 2.1.	Channel Characteristics and Cation Sites in Clinoptilolite.....	6
Table 3.1.	Properties of some adsorbate gases.....	13
Table 4.1.	Previous Studies involving IAS Theory.....	32
Table 5.1.	Adsorbents used in the study.....	33
Table 5.2.	Adsorption characteristics of the adsorbents studied.....	34
Table 6.1.	Maximum adsorption capacities of zeolites at 50C and 250C for CO ₂ Adsorption.....	44
Table 6.2.	Maximum adsorption capacities of zeolites at 5 ⁰ C and 25 ⁰ C for N ₂ Adsorption.....	45
Table 6.3.	Previous Studies of N ₂ and CO ₂ Adsorption on Zeolites	46
Table 6.4.	Langmuir Parameters of the Zeolites at 5 ⁰ C and 25 ⁰ C for CO ₂	47
Table 6.5.	Langmuir Parameters of the samples at 5 ⁰ C and 25 ⁰ C for N ₂ Adsorption.....	48
Table 6.6.	Sips Parameters of the Zeolites at 5 ⁰ C and 25 ⁰ C for CO ₂ Adsorption.....	49
Table 6.7.	Sips Parameters of the Zeolites at 5 ⁰ C and 25 ⁰ C for N ₂ Adsorption.....	50
Table 6.8.	Henry's Constants for the CO ₂ and N ₂ Adsorption at 5 ⁰ C and 25 ⁰ C	53
Table 6.9.	Selectivity Ratios of CO ₂ over N ₂ for the Adsorbents at 5 ⁰ C and 25 ⁰ C.....	54
Table 6.10.	Comparison of the heat of adsorption values of the zeolites at zero coverage	69
Table 6.11.	Heat of adsorption values of CO ₂ and N ₂ on zeolites.....	72

CHAPTER 1

INTRODUCTION

Separation is based on the selective adsorption of one or more components of a feed gas mixture on to a solid adsorbent in order to produce a gas stream which is enriched in the less strongly adsorbed components, followed by desorption of the adsorbed components in order to clean the adsorbent for re-use.

The separation and purification of gas mixtures by adsorption has found numerous commercial applications in the chemical, petrochemical, environmental, medical and electronic gas industries. These applications can be divided broadly into the following two categories; (a) the removal of trace or dilute impurities from a gaseous mixture and (b) the bulk separation of gaseous mixtures. In bulk separation more than 10 % by weight from a gas stream is adsorbed while in purification process less than 10 % by weight of a gas stream is adsorbed. Included among the many possible commercial applications of natural zeolites are gas purification, drying and bulk separations. The adsorption properties of clinoptilolite and its ion-exchange derivatives have been investigated for many applications such as natural gas purification and drying (removal of CO₂, H₂S, N₂ and H₂O), air separation (both O₂ and N₂ production), flue gas cleanup (SO₂ removal), and in coal gasification (NH₃ removal).

Clinoptilolite is a member of the heulandite group of natural zeolites and it is the most abundant natural zeolite however remains largely uncommercialized for gas separation processes due to variation in the purity and composition of the various mineral deposits. Besides, low cost, ready availability, and versatility of synthetic zeolites has inhibited the commercialization of natural zeolites.

In literature different methods are stated for purification purposes of natural zeolites. The most common one is to wash the natural zeolite with deionized water. Another method is to settle down the heavy impurities due to density difference using s-tetrabromoethane and acetone mixture (Roberts, 1995). Impurities can be also removed by heating the natural zeolite in distilled water then dispersing in methyl iodide (Ackley et al., 1991). Purification process due to acid treatment also increases the adsorption capacity because it increases the surface area of clinoptilolite and also the Si/Al ratio due to dealumination. Consequently, electric field on the surface

decreases due to removal of polar cations from the surface. This also increases the hydrophobicity of the surface (Yang, 1987).

In this work, the heats of adsorption and adsorption isotherms of CO₂, N₂ and Ar gases on natural zeolites treated with different acid concentrations and on synthetic zeolites of 13X and 5A were investigated.

From the adsorption data the interaction parameters were determined using some model equations in order to investigate the change in the energetic heterogeneity of the zeolites due to dealumination.

Besides, by making use of data obtained from volumetric studies at 5 and 25⁰C, isosteric heat of adsorptions were calculated theoretically and compared with the data obtained experimentally from calorimetric studies.

CHAPTER 2

ZEOLITES

2.1 Definition

Zeolites form a family of minerals, which have been known since 18th century, but they remained a curiosity for scientists and collectors until 60 years ago, when their unique physicochemical properties attracted the attention of many researchers.

Zeolites are porous crystalline aluminosilicates. The zeolite framework consists of an assemblage of SiO₄ and AlO₄ tetrahedra, joined together in various regular arrangements through shared oxygen atoms to form an open crystal lattice containing pores of molecular dimensions into which molecules can penetrate.

There are more than 50 different available types of aluminosilicate zeolites with pore openings ranging from less than 5 Å to larger than 10 Å (Webster et al., 1999). These porous, crystalline, hydrated aluminosilicates of alkali and alkaline earth cations possess a three dimensional structure. The negative charge created by the substitution of an AlO₄ tetrahedron for a SiO₄ tetrahedron is balanced by exchangeable cations (e.g., Na⁺, K⁺, Ca²⁺, Mg²⁺), which are located in large structural channels and cavities throughout the structure. These cations play a very important role in determining the adsorption and gas-separation properties of zeolites. These properties depend heavily on the size, charge density, and distribution of cations in the porous structure. These natural minerals are found with a Si/Al ratio ranging between 3 and 5 (Zhao et al., 1998).

Synthetic zeolites are manufactured on a large scale for industrial use, but natural zeolites have not yet found extensive application as commercial molecular sieves, even though a few, particularly clinoptilolite are abundant in volcanogenic sedimentary rocks. Of the more than 40 natural zeolites species known today, clinoptilolite is the most abundant in soils and sediments (Armenta et al., 2001).

2.2. Structure

Like most silicates the zeolites are based on TO_4 tetrahedra, where T is an aluminium or silicon atom. The vast 3-dimensional networks are a result of all four corners for the tetrahedra being shared, producing low density microporous materials. Zeolite structures can be thought to exist of finite or infinite (chains, layers etc..) component units.

The finite units which have been found to occur are shown in the figure below

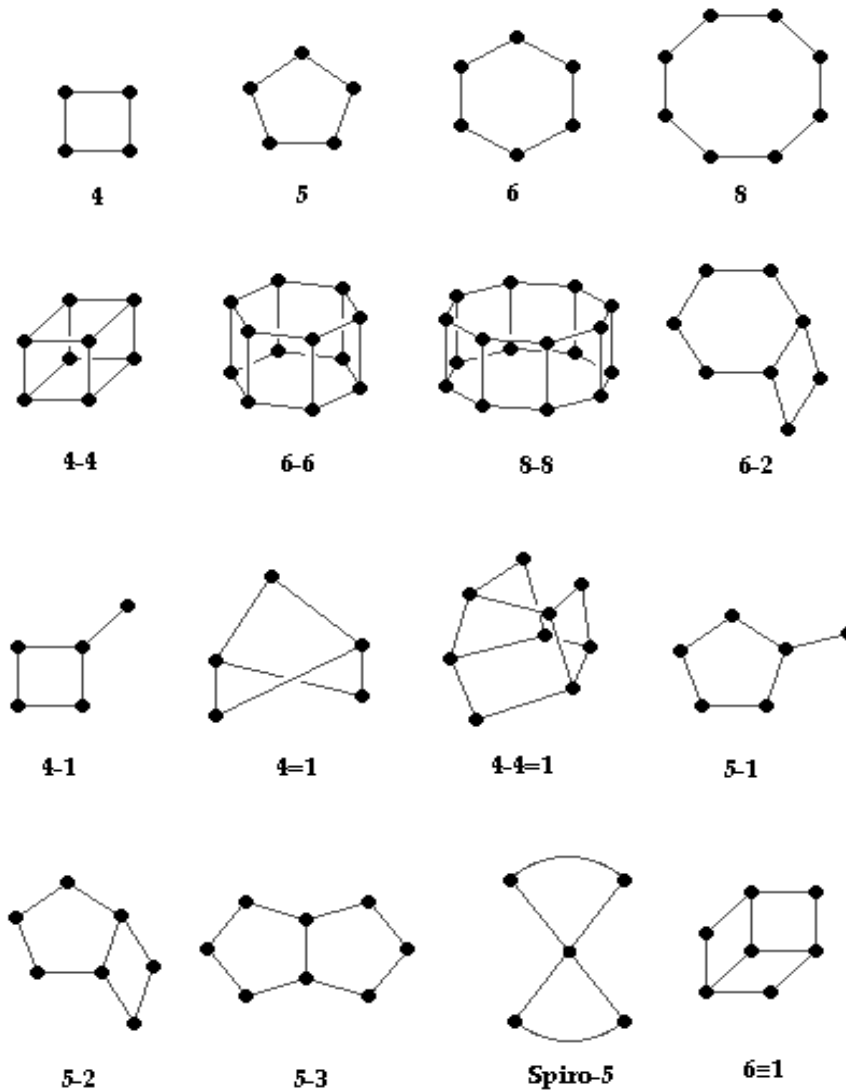


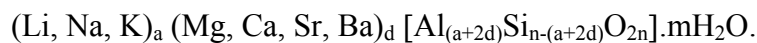
Figure 2.1: Secondary Building Units (SBU's) in zeolites. The corner of the polyhedra represent tetrahedral atoms.

2.3 Clinoptilolite-rich Natural Zeolite

Clinoptilolite is the most common natural zeolite found mainly in sedimentary rocks of volcanic origin. Such deposits aroused strong commercial interest because clinoptilolite tuffs are often rather pure and can be mined with simple techniques. Approximately 25 years ago 300.000 tons of zeolitic tuff was mined per year. In 1997, 3.6 million tons of natural zeolites (mainly clinoptilolite and chabazite) were worldwide produced. Demand for natural zeolites has increased rapidly over the past decade, particularly in agricultural applications. Growth rates as high as 10% per year are forecasted (Galarnau et al., 2001).

Commercially available natural zeolites are usually of the clinoptilolite variety which are known chemically as hydrated sodium calcium aluminosilicates. Clinoptilolite's unique crystalline structure and extraordinary properties are present, regardless of the particle size. This structure never breaks down under extreme pressures, requires temperatures that melt glass to break down and it cannot be chemically changed except under extremely caustic or acid conditions. Degradation over time is impossible without one of the above conditions being present (Woldegabriel et al., 1992).

Clinoptilolite is a member of the heulandite group of natural zeolites and has a similar structure with the zeolite heulandite. The general formula for natural zeolites is:



The unit cell is monoclinic C-centered and is usually characterized on the basis of 72 Oxygen atoms ($n = 36$) and $m = 24$ water molecules with Na^+ , K^+ , Ca^{2+} , and Mg^{2+} as the most common charge balancing cations.

This 2-D microporous channel system was first characterized for heulandite. Channels A (10-member ring) and B (8-member ring) are parallel to each other and the c-axis of the unit cell, while the C channel (8-member ring) lies along the a-axis intersecting both the A and B channels as shown in Figure 2.3. (Ackley et al., 1992).

Small hydrated cations (Na^+ , K^+ , Ca^{2+} , Mg^{2+}) can easily enter the channels of clinoptilolite and compete for the major exchangeable-cation sites designated as M(1), M(2), M(3), and M(4). The major cations are located and distributed as follows;

M(1) is located in channel A, where $\text{Na} > \text{Ca}$, M(2) is located in channel B, where $\text{Ca} > \text{Na}$, M(3) is located in channel C, where there is only K and M(4) is located in channel A, where there is only Mg. These properties of clinoptilolite are presented in table 2.1. The cation positions in the clinoptilolite structure are shown in Figure 2.2.

Table 2.1: Channel Characteristics and Cation Sites in Clinoptilolite

Channel	tetrahedral ring size/channel axis	cation site	major cations	Approximate channel dimensions, nm×nm
A	10/c	M(1)	Na, Ca	0.72×0.44
B	8/c	M(2)	Ca, Na	0.47×0.41
C	8/a	M(3)	K	0.55×0.40
A	10/c	M(4)	Mg	0.72×0.44

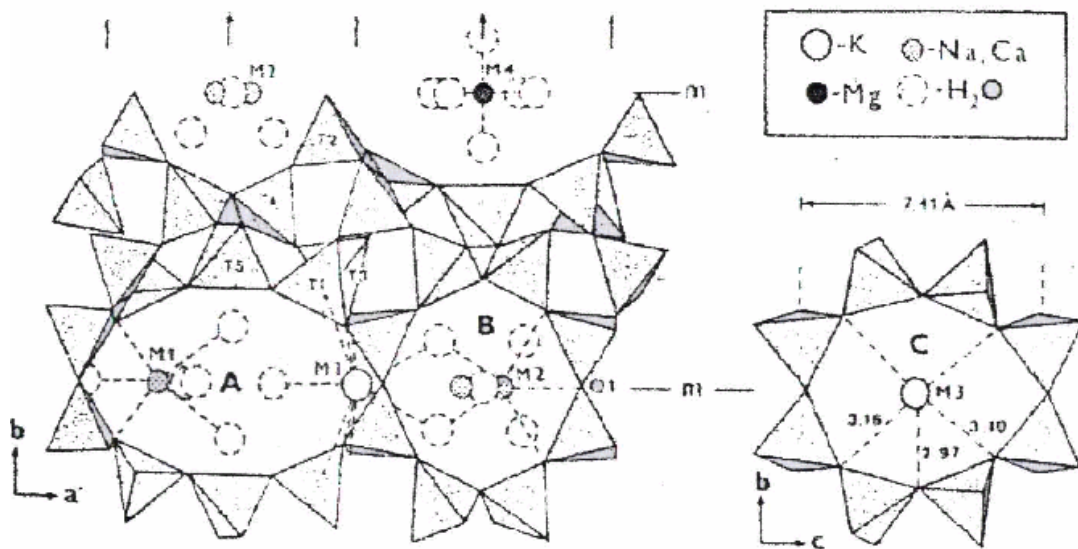


Figure 2.2: The c-axis projection of the structure of clinoptilolite, showing the cation positions in the structure.

The composition of the heulandite-clinoptilolite series is characterized by remarkable changes in the Si/Al ratio as well as in the composition of exchangeable cations. Numerous statistical treatments of published chemical analyses have revealed clear correlations; as a rule, low silica members are enriched with calcium and often contain Ba and Sr, whereas high silica species are enriched with potassium, sodium and magnesium. In literature, high silica clinoptilolite is called simply clinoptilolite, whereas low silica varieties are known as Ca-clinoptilolite. Such a classification is closely associated with optical, thermal and other properties of the zeolites.

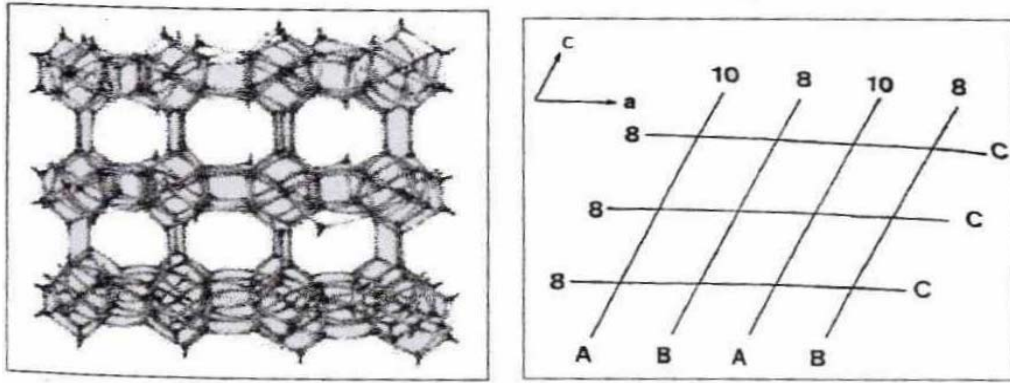


Figure 2.3: Schematic diagram of clinoptilolite structure

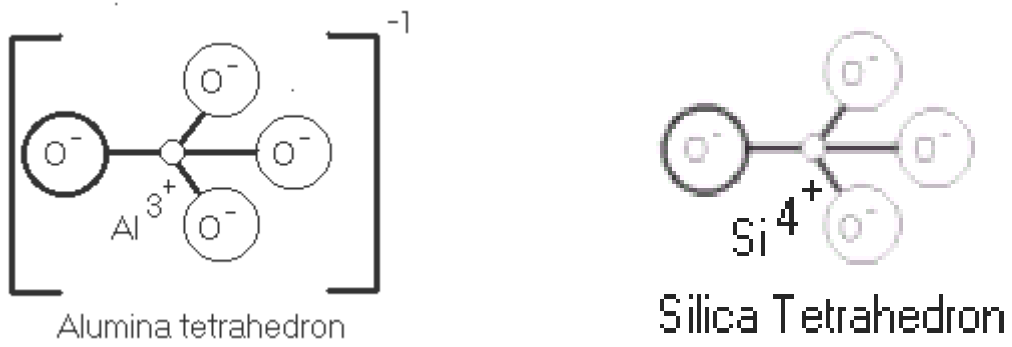


Figure 2.4: Center occupied by Si^{+4} or Al^{+3} atom with four O atoms at the corners

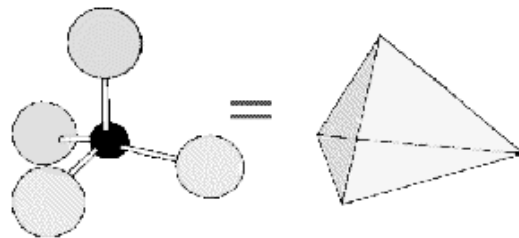


Figure 2.5: Tetrahedron-primary building unit

2.4 Synthetic Zeolites

Zeolite A

The simplest synthetic zeolite is the zeolite A with a molecular ratio of one silica to one alumina to one sodium cation. The zeolite A synthesis produces precisely duplicated sodalite units which have 47% open space, ion exchangeable sodium, water of hydration and electronically charged pores. These properties lead to the various uses of natural and synthetic zeolites.

The aluminosilicate framework of zeolite A can be described in terms of two types of polyhedra; one is a simple cubic arrangement of eight tetrahedra and the other is the truncated octahedron of 24 tetrahedra or β -cage. The aluminosilicate framework of zeolite A is generated by placing the cubic D4R units ($\text{Al}_4\text{Si}_4\text{O}_{16}$) in the centers of the edges of a cube of edge 12.3Å. This arrangement produces truncated octahedral units centered at the corners of the cube. Each corner of the cube is occupied by a truncated octahedron (β -cage) enclosing a cavity with a free diameter of 6.6 Å. The center of the unit cell is a large cavity, referred to as the α -cage, occupy the apices of a truncated cuboctahedron.

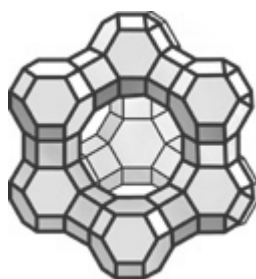
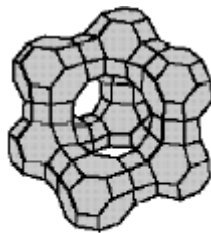


Figure 2.6: Structure of Zeolite A

The unit cell of zeolite A contains 24 tetrahedra, 12 AlO_4 and 12 SiO_4 . When fully hydrated, there are 27 water molecules. The electrostatic valance rule requires an alternation of the AlO_4 and SiO_4 tetrahedra, because the Si/Al ratio is 1:1. Normally, zeolite A is synthesized in the Na-form. Other cationic forms are easily prepared by ion exchange in aqueous solution (Breck, 1973).

Zeolite X and Y

The faujasite-type zeolites all have the same framework structure as indicated in Figure 2.7. The general composition of the unit cell of faujasite is $(\text{Na}_2, \text{Ca}, \text{Mg})_{29}[\text{Al}_{58}\text{Si}_{134}\text{O}_{384}].240\text{H}_2\text{O}$. The SBU's are double six rings and the FD is 12.7 nm^{-3} . The unit cell contains eight cavities, each of diameter $\approx 13 \text{ \AA}$. The three dimensional channels which run parallel to $[110]$, have 12 ring windows with free apertures of about 7.4 \AA . The difference between zeolites X and Y is in their Si/Al ratios which are 1-1.5 and 1.5-3, respectively (Sing et. al., 1999).



X, Y

Figure 2.7: Structure of X and Y synthetic zeolites

2.5 Uses and Applications

The family of zeolites containing the heulandite is the most abundant zeolites found in nature. Zeolites are classified into groups according to common features of the aluminosilicate framework structures. The properties which are structure related are;

- High degree of hydration and the behaviour of zeolitic water
- Cation exchange properties
- Uniform molecular-sized channels in the dehydrated crystals
- Adsorption of gases and vapors
- Catalytic properties
- Stability of the crystal structure of many zeolites when dehydrated

The framework structures of the zeolites are composed of assemblages of tetrahedra in building units which range from simple 4-rings to large polyhedra (Breck, 1973). Due to its superior structure properties clinoptilolite has many industrial applications. It's been applied to gas and radioactive wastewater

cleaning, gas separation, and gas drying and also to separate O₂ from air. It's noted that natural zeolites, primarily chabazite and clinoptilolite have been used to purify natural gas contaminated with large amounts of CO₂, H₂S and H₂O (Armenta et al., 2001).

The discovery of natural zeolites 40 years ago as large, widespread, mineable, near-monomineralic deposits in tuffaceous sedimentary rocks in the western United States and other countries opened another chapter in the book of useful industrial minerals whose exciting surface and structural properties have been exploited in industrial, agricultural, environmental, and biological technology. Like talc, diatomite, wollastonite, chrysotile, vermiculite, and bentonite, zeolite minerals possess attractive adsorption, cation-exchange, dehydration–rehydration, and catalysis properties, which contribute directly to their use in pozzolanic cement; as lightweight aggregates; in the drying of acid-gases; in the separation of oxygen from air; in the removal of NH₃ from drinking water and municipal wastewater; in the extraction of Cs and Sr from nuclear wastes and the mitigation of radioactive fallout; as dietary supplements to improve animal production; as soil amendments to improve cation-exchange capacities (CEC) and water sorption capacities; as soilless zeoponic substrate for greenhouses and space missions; in the deodorization of animal litter, barns, ash trays, refrigerators, and athletic footwear; in the removal of ammoniacal nitrogen from saline hemodialysis solutions; and as bactericides, insecticides, and antacids for people and animals. This multitude of uses of natural zeolites has prompted newspapers in Cuba, where large deposits have been discovered, to refer to zeolites as the magic rock. Included among the many possible commercial applications of natural zeolites are gas purification, drying and bulk separations (Ackley et al., 1992).

Due to possessing of different useful properties of natural zeolites, they have very important uses also in pollution control, the handling and storage of nuclear wastes, agriculture, and biotechnology. Natural zeolites are also involved by mineral scientists for greater involvement in the surface, colloidal, and biochemical investigations that are needed in the future development of zeolite applications (Mumpton, 1999).

CHAPTER 3

ADSORPTION

3.1 Definition

Adsorption occurs whenever a solid surface is exposed to a gas or liquid and it is defined as the enrichment of material or increase in the density of the fluid in the vicinity of the interface. The term adsorption may also be used to denote the process in which adsorptive molecules are transferred to, and accumulate in, the interfacial layer. Its counterpart desorption, denotes the converse process in which the amount adsorbed decreases. Based on the nature of the bonding between the adsorbate molecule and the solid surface, adsorption can be categorized as either physical adsorption, which doesn't involve chemical bonding or chemisorption which involves chemical bonding.

Adsorption is of great importance. The unique advantage of adsorption over other separation methods is the higher selectivity that can be achieved by adsorbents. In addition, adsorption phenomena play a vital role in many solid state reactions and biological mechanisms.

There are many industrial applications of adsorption. The most significant commercial adsorption-related applications in industry are the purification of acid natural gas streams, gas drying, ammonia removal from gases, air separation and deodorization (Ruthven D.M., 1984).

3.2 Adsorbents

In the adsorption process, adsorbent is an additional component, which plays the crucial role. It is the solid material on which adsorption occurs. Commercially useful adsorbents can be classified by the nature of their structure (amorphous or crystalline), by the sizes of their pores (micropores, mesopores, and macropores), by the nature of their surfaces (polar, nonpolar or intermediate), or by their chemical composition. All of these characteristics are important in the selection of the best adsorbent for any particular application (Ruthven D.M., 1984).

Some adsorbents are used on large scale as dessicants, catalysts or catalyst supports while others are used for the separation of gases, the purification of liquids, pollution control or for respiratory protection. There are different adsorbents being

used in industry such as Active Carbon, silica gel, silicalites, activated clays, synthetic zeolites, natural zeolites (Clinoptilolite, Erionite, Mordenite), 4A, 5A, 13X molecular sieves, activated aluminas.

For an adsorption process to be developed on a commercial scale requires the availability of a suitable adsorbent in tonnage quantities at economic cost. This led to the fundamental research in adsorption consequently to the development of new adsorbents. The earlier adsorption processes used either activated carbon or silica gel adsorbents but the potential of adsorption as a separation process was greatly enhanced by the development of molecular sieve adsorbents such as natural and synthetic zeolites.

In this study, clinoptilolite from Gördes region, which is a natural zeolite as well as 5A and 13X synthetic zeolites were used as the adsorbents. The properties of these materials are extremely important in order to predict the results, which will be obtained throughout the experiments. In table 3.1., the properties of the adsorbate gases used in adsorption processes for the comparison purposes are presented.

Table 3.1: Properties of some adsorbate gases

Adsorbate	Mol. Wt.	Kinetic Diameter (Å)	Polarizability ($\times 10^{-25}$ cc)	Permanent dipoles	
				Dipole ($\times 10^{-18}$ esu)	Quadrupole ($\times 10^{-26}$ esu-cm ²)
N ₂	28	3.64	15.8	0	1.52
Ar	40	3.4	16.3	0	-
O ₂	32	3.46	17.6	0	0.39
CO	28	3.76	19.5	0.112	2.50
CO ₂	44	3.30	26.5	0	4.30
CH ₄	16	3.80	26.0	0	0
C ₂ H ₆	30	4.44	44.7	0	1.50
C ₂ H ₄	28	3.90	42.6	0	0.65
C ₃ H ₈	44	4.30	62.9	0.084	
C ₃ H ₆	42	4.68	57.4	0.366	
C ₄ H ₁₀	58	5.00	82.0	0.132	

3.3 Properties of the Adsorbate Gases Used in this Study

Adsorbates used in this study are CO₂, N₂, Ar and their properties are given in Table 3.1.

3.3.1. Carbondioxide

- It has high quadrupole moment meaning that its adsorption isotherm is very sensitive to the presence of polar groups or ions in the surface of the solid
- CO₂ cannot be recommended for routine determinations of specific surface. It's hard to desorb CO₂ since it is too small, besides possibility of chemisorption is a complicating factor. On the other hand, it should be particularly suitable for the study of the polarity of surfaces in systems where chemisorption can be excluded from consideration.
- Sensitivity to surface polarity causes wide variation in molecular cross-sectional area values for CO₂
- CO₂ adsorption at subatmospheric pressures is a useful complementary technique for the characterization of very narrow micropores and that at higher pressures the adsorption of CO₂ is similar to N₂.
- For carbondioxide two effects are shown: (1) a high initial adsorption heat characteristic of the quadrupole interaction followed by (2) a minimum and a maximum with increased loading. The increase in isosteric heat is due to interaction between the adsorbate molecules.

3.3.2. Nitrogen

- N₂ molecule is diatomic and it is a non-spherical molecule.
- Quadrupole moment of this molecule leads to localized adsorption on polar sites and provides a well defined monolayer on most surfaces.
- The adsorption behaviour of N₂ on ion exchanged zeolites correlates with the cation distribution, because the interaction between the quadrupole moment of nitrogen and the electrostatic field of the cations plays an important role in adsorption.
- For evaluation of both the surface area and the pore size distribution of a solid from a single isotherm, nitrogen is the most suitable adsorptive. The use of other

adsorptives is not recommended except for the study of the structure of the surface or as molecular probes for evaluation of micropore size.

3.3.3. Argon

- It's chemically inert
- Its molecule is symmetrical and monoatomic.
- Although the polarizabilities of Argon and nitrogen are remarkably similar, their electronic structures are quite different.
- Argon is a possible alternative adsorptive for surface area determination (Sing et al., 1999.).

3.4 Pure Gas Adsorption Isotherms

Adsorption isotherm is the relationship between the amount of gas adsorbed and pressure or relative pressure at constant temperature. A useful indication of the mechanisms of surface coverage and/or pore filling can be obtained by visual inspection of an isotherm. The overall shape of an isotherm is governed by the nature of the gas-solid system, the pore structure of the adsorbent and the operational temperature.

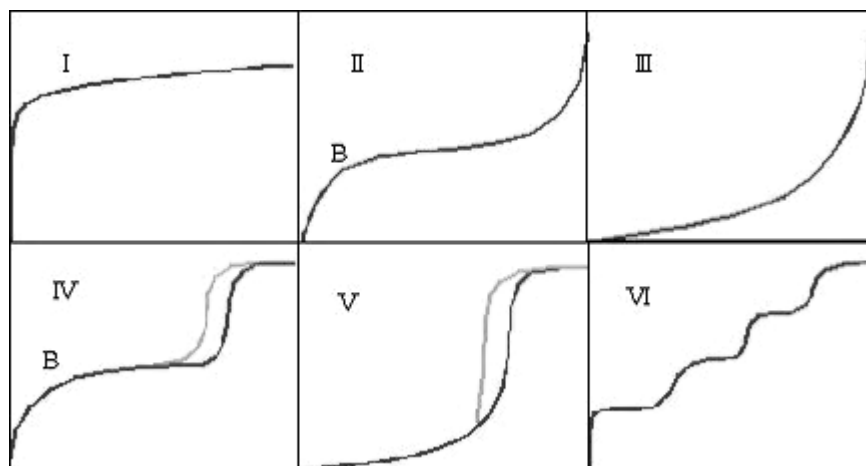


Figure 3.1: The six main types of gas physisorption isotherms

The majority of physisorption isotherms may be grouped into six types according to IUPAC classification. In most cases at sufficiently low surface coverage

the isotherm reduces to a linear form, which is often referred to as Henry's Law Region.

The main feature of a Type I isotherm is the long plateau, which is indicative of a relatively small amount of multilayer adsorption on the open surface. Micropore filling may take place either in pores of molecular dimensions at very low p/p° or in wider micropores over a range of higher p/p° .

A type II isotherm is normally associated with monolayer-multilayer adsorption on an open and stable external surface of a powder, which may be non-porous, macroporous or even to a limited extent microporous.

Type III isotherms are confined to a few systems in which the overall adsorbent-adsorbate interactions are weak in comparison with relatively strong adsorbate-adsorbate interactions. Isotherms of this kind are not common.

Characteristic features of the type IV isotherm are its hysteresis loop, which is associated with capillary condensation taking place in mesopores, and the limiting uptake over a range of high p/p° .

The type V isotherm is uncommon; it is related to the type III isotherm in that the adsorbent-adsorbate interaction is weak but is obtained with certain porous adsorbents.

The type VI isotherm, in which the sharpness of the steps depends on the system and the temperature, represents stepwise multilayer adsorption on a uniform non-porous surface. Among the best examples of type VI isotherms are those obtained with argon or krypton on graphitized carbon blacks at liquid nitrogen temperature.

There are some models which help characterizing the adsorbent to see if the adsorbent has the desired properties for a certain application. The interaction parameters of these models indicate the extent of heterogeneity of the adsorbent being investigated. In this study, the interaction parameters of the acid treated natural zeolites have been determined by using the models stated in this chapter.

3.4.1. Langmuir Model

The simplest theoretical model for monolayer adsorption is due to the Langmuir model. The basic assumptions on which the model is based on are as follows;

1. Molecules are adsorbed at a fixed number of well-defined localized sites.

2. Each site can hold one adsorbate molecule.
3. All sites are energetically equal.
4. There is no interaction between molecules adsorbed on neighbouring sites.

The Langmuir adsorption method is still the most widely used procedure for the determination of the surface area of porous materials. The Langmuir equation is

$$\theta = \frac{n}{n_m} = \frac{bP}{1+bP} \quad (3.1)$$

where θ is the monolayer coverage (n is the amount adsorbed in mmol per unit mass or volume and n_m is the maximum adsorbed concentration corresponding to a complete monolayer coverage).

$1/n$ vs $1/P$ graph gives Langmuir plot. From slope and intercept, b and n_m values are calculated respectively. (Sing, 1999).

Parameter b is called the affinity constant or Langmuir constant. It is a measure of how strong an adsorbate molecule is attracted onto a surface. When the affinity constant b is larger, the surface is covered more with adsorbate molecule as a result of the stronger affinity of adsorbate molecule towards the surface. Besides, increase in temperature decreases the amount adsorbed at a given pressure. This is due to the greater energy acquired by the adsorbed molecule to evaporate (Do D., 1998).

3.4.2. Dubinin Models

In characterizing the microporous solids, evaluation of the parameters that characterize the microporous structure is an important problem. Dubinin and Radushkevich proposed an equation for describing the physical adsorption of gases on microporous solids. Adsorption of molecule in surfaces having constant energy of interaction is very rare in practice as most solids are very heterogeneous. Therefore the degree of heterogeneity is determined by assuming that the energy of interaction between the surface and the adsorbing molecule is governed by some distribution (Do et al., 1999).

Dubinin and Radushkevich proposed an equation for describing the physical adsorption of gases and vapors on microporous solids. This equation is one of the

most popular isotherm equations in adsorption theory, and has been widely used to describe the experimental data of adsorption of gases on microporous adsorbents. Several workers postulated that the DR equation applies only to solids with a uniform structure of micropores (Gil et al., 1996).

Dubinin Radushkevitch is expressed as;

$$\theta = V/V_0 = \exp[-(B(T/\beta)^n \log^n(P_0/P))] \quad (3.2)$$

where θ is the relative adsorption, which is defined as the ratio of the amount adsorbed in the micropores (V) to the maximum micropore adsorption capacity (V_0). In this equation B is termed the structural constant and β is termed the convergence coefficient of the characteristic curves (Gil et al., 1996).

Various possible equations have been proposed for adsorbents with a nonhomogeneous micropore structure. One of them is Dubinin Astakhov equation. This equation has been used to describe the energetic heterogeneity of the solids. DA expression can be applied to the description of the adsorption on structurally heterogeneous solids

Dubinin Astokhov equation is expressed as;

$$\theta = V/V_0 = \exp[-(A/E)^n] \quad (3.3)$$

In this equation E denotes characteristic energy and A is the adsorption potential. In these equations the term n has been referred to as a “heterogeneity factor” and it has been suggested that it is related in some way to the heterogeneity of the surface (Nick et al., 1996). Dubinin Astakhov expression can be applied to the description of the adsorption on structurally heterogeneous solids while For this equation the exponent n is usually taken as 2 while for Dubinin Astakhov equation n is generally taken 3 for microporous adsorbents (Gil et al. 1996).

3.4.3. Empirical Isotherm Equations

Many different equations have been applied to physisorption isotherms on microporous adsorbents. The first and best known empirical equation was proposed by Freundlich in the form

$$n = kp^{1/m} \quad (3.4)$$

where k and m are constants ($m > 1$). According to Freundlich equation the plot of $\ln [n]$ against $\ln [p]$ should be linear. In general, adsorbents give isotherms which obey the Freundlich equation in the middle range of pressure, but the agreement is usually poor at high pressures and low temperatures. These limitations are due to the fact that the Freundlich isotherm does not give a limiting value of n as $p \rightarrow \infty$

Another empirical variant is Toth equation,

$$n/n_m = \frac{p}{(b + p^m)^{1/m}} \quad (3.5)$$

which also contains three adjustable parameters (n_m , b and m) but has the advantage that it appears to give the correct limits for both $p \rightarrow 0$ and $p \rightarrow \infty$. Therefore Toth equation gives a more extensive range of fit when applied to type I isotherms (Do, 1999).

Another model applied to represent the experimental data is the Sips model.

$$\frac{n}{n_m} = \frac{(bP)^{\frac{1}{t}}}{1 + (bP)^{\frac{1}{t}}} \quad (3.6)$$

The difference between this equation and the Langmuir equation is the additional parameter “ t ”. If this parameter is unity, Sips equation is reduced to Langmuir equation which can be applied for ideal surfaces. Hence the parameter t could be regarded as the parameter characterizing the system heterogeneity. The system heterogeneity could be result of the solid or the adsorbate or a combination of

both. The parameter t is usually greater than unity, and therefore the larger is this parameter the more heterogeneous is the system.

Virial Model provides a general method of analyzing the low coverage region of an adsorption isotherm and its application is not restricted to particular mechanisms or systems.

$$p = n \exp(C_1 + C_2 n + C_3 n^2) \quad (3.7)$$

where the coefficients (C_1, C_2, C_3) are characteristic constants for a given gas-solid system and temperature. The linear form of the equation is:

$$\ln\left(\frac{n}{P}\right) = K_1 + K_2 n + K_3 n^2 + \dots \quad (3.8)$$

Thus the intercept of the virial plot of $\ln(n/p)$ versus n , it is possible to obtain Henry's constant, k_H , since

$$k_H = \lim_{p \rightarrow 0} (n/p) \quad (3.9)$$

Therefore, K_1 is directly related to k_H and to the gas-solid interaction (Sing K., 1999).

Henry's constants determined from the Virial plot of $\ln(p/n)$ vs n are also presented and they indicate the the interaction parameter of the gas molecule with the adsorbent surface . It is stated in literature that at low surface coverage, adsorption isotherm of a pure gas on a homogeneous adsorbent reduces to Henry's Law and is a function of pressure in the very low pressure (Cao et al., 2001).

3.4.4. Henry's Law

The simplest interpretation of the behavior of the adsorbed phase is to suppose that, at very low surface excess concentration, the adsorbate molecules are independent of each other. By assuming that the dilute adsorbed phase behaves as a two-dimensional ideal gas, regardless of the nature of the adsorption, the final Henry's equation can be expressed as;

$$n = k_h p \quad (3.10)$$

where n is used to represent the specific surface excess amount and k_h is generally known as the Henry's Law constant. Thus, at sufficiently high temperatures and sufficiently low pressures, n , should vary linearly with the equilibrium gas pressure. (Sing, 1999).

By making use of the pure gas data obtained from experimental studies and the single gas models appropriate for these data which have been stated in this chapter, mixed gas data can be predicted. Correlations for mixed-gas adsorption are important to the design of adsorptive gas separation processes. They should be capable of predicting the equilibrium amount adsorbed from pure gas isotherms for each constituent in the mixture, within given ranges of operating temperature and total pressure.

The measurement of mixed gas adsorption is not very difficult but it is rather long. With the additional measurement of equilibrium gas phase composition, nearly all experimental techniques used for measuring single gas isotherms can be used for mixed gas adsorption. For example the Langmuir isotherm for single gas adsorption can readily be extended to an n -component mixture, and the surface coverage of species i for an n -component mixture is given as: $\theta_i = B_i P_i / (1 + \sum B_j P_j)$ where j is from 1 to n .

Several studies have been published which proposes methods for predicting multicomponent adsorption equilibria utilizing parameters from an empirical isotherm equation such as the Langmuir, Freundlich equations, etc. that characterize single component adsorption equilibria and comparisons with other methods such as IAST, Polanyi Dubinin theory. The prediction of multicomponent adsorption equilibria from single component data is one of the most challenging and important problems in adsorption.

Ideal adsorbed solution theory (IAST) is being used extensively to predict binary gas mixture systems by making use of the single gas adsorption data. IAST is a very popular and thermodynamically consistent predictive method. IAST uses an isotherm equation such as Langmuir, to represent the single component isotherms (Yang, 1987).

CHAPTER 4

GAS SEPARATION

4.1. Factors Affecting Separation

There are several factors affecting separation of the gas mixtures. Those factors have to be taken into consideration when dealing with the adsorption processes.

4.1.1. Adsorbent and Adsorbate Interactions

The total potential energy of adsorption interaction may be subdivided into parts representing contributions of the different types of interactions between adsorbed molecules and adsorbents. The total energy ϕ_{total} is the sum of contributions resulting from dispersion energy ϕ_{D} , close-range repulsion ϕ_{R} , polarization energy ϕ_{P} , field-dipole interaction $\phi_{\text{F-}\mu}$, field gradient-quadrupole interaction $\phi_{\delta \text{ F-Q}}$, and adsorbate-adsorbate interactions, denoted self potential ϕ_{SP} ;

$$\phi_{\text{total}} = \phi_{\text{D}} + \phi_{\text{R}} + \phi_{\text{P}} + \phi_{\text{F-}\mu} + \phi_{\delta \text{ F-Q}} + \phi_{\text{SP}} \quad (4.1)$$

The ϕ_{D} and ϕ_{R} terms always contribute, regardless of the specific electric charge distributions in the adsorbate molecules, which is why they are called nonspecific. The third nonspecific ϕ_{P} term also always contributes whether or not the adsorbate molecules have permanent dipoles or quadrupoles; however for adsorbent surfaces which are relatively nonpolar, the polarization energy ϕ_{P} is small.

The $\phi_{\text{F-}\mu} + \phi_{\delta \text{ F-Q}}$ terms are specific contributions, which are significant when adsorbate molecules possess permanent dipole and quadrupole moments. In the absence of these moments, these terms are zero, as is true also if the adsorbent surface has no electric fields, a completely nonpolar adsorbent.

Finally, the ϕ_{SP} is the contribution resulting from interactions between adsorbate molecules. At low coverages of the adsorbent by adsorbate molecules, this contribution approaches zero, and at high coverage it often causes a noticeable increase in the heat of adsorption.

These contributions to the potential energy of adsorption are present even if the adsorbed molecules are nonpolar and even if the adsorbent structure contains no strong electrostatic field. The contribution ϕ_p is due to the polarization of the molecules by electric fields on the adsorbent surface such as electric fields between positively charged cations and the negatively charged framework of a zeolite adsorbent. The attractive interaction between the induced dipole and the electric field is called the polarization contribution (Ruthven, 1984).

4.1.2. Surface structure of the adsorbent

In the crystalline adsorbents such as zeolites and microporous aluminum phosphates, the dimensions of the micropores are determined by the crystal framework and there is therefore virtually no distribution of pore size. The crystals of these materials are generally quite small (1-5 μm) and they are aggregated with a suitable binder and formed into macroporous particles having dimensions large enough to pack directly into an adsorber vessel. Such materials therefore have a well defined bimodal pore size distribution with the intracrystalline micropores linked together through a network of macropores having a diameter of the same order as the crystal size (Ruthven, 1984).

Surface structure of natural zeolites is usually heterogeneous which means that it consists of a finite number of different kinds of adsorption sites and due to heterogeneity of the surface of natural zeolites, there occur different gas selectivities on different parts of the surface, which cause deviations in model predictions (Karacan et al., 1999).

Dealumination

Zeolites can be dealuminated using different procedures such as extraction with EDTA, high temperature steaming, reaction with SiCl_4 , or substitution with $(\text{NH}_4)_2 \text{SiF}_6$. These procedures can be followed by acid leaching to remove the nonframework aluminum (Solinas et al., 1998). Acid washing of small pore natural zeolites may remove impurities that block the pores, progressively eliminate cations and finally dealuminate the structure as the strength and duration of the treatment increases. In clinoptilolite, acid treatment can increase both porosity and adsorption capacity, improve adsorption of acid gases and extend adsorbent life (Ackley, 2002).

Hydrophilic and Hydrophobic Surfaces

The key physical property of every adsorbent is the surface hydrophobicity (Sakut M., 1998). Adsorbents which have a polar surface and therefore adsorb highly polar molecules such as H₂O are called hydrophilic. In contrast, on a nonpolar surface where there is no electrostatic interaction usually adsorb nonpolar molecules and water is held only very weakly on the surface of the adsorbent which are termed hydrophobic (Ruthven, Adsorption, Gas separation). In zeolitic adsorbent hydrophobicity can be varied by changing the Silicon to Aluminum ratio. For example the surface of zeolites usually exhibits polar and nonpolar adsorption behavior depending on the degree of dealumination. Highly dealuminated zeolites preferably adsorb nonpolar compounds from mixtures of adsorptives with different polarities (Sakut et al., 1998). Adsorption systems include a large variety of polar and nonpolar adsorbates of different molecular sizes that are adsorbed on various microporous homogeneous and heterogeneous adsorbents of practical interest (Rao, 1999).

Cationic density (Si/Al ratio) of the adsorbent

Different cationic forms of a given zeolite may lead to significant differences in the selective adsorption of a given gas, due to both the location and size of the interchangeable cations which affect the local electrostatic field, and polarization of the adsorbates. The relative adsorption capacities of natural zeolites over the entire equilibrium pressure range are related to two factors which are;

- the number of cations available per unit mass of the dehydrated zeolites (cationic density)
- the limiting volume of the micropore (Hernandez et al., 1998).

When the Si/Al ratio is increased which means that when the zeolite is dealuminated, the electrostatic field on the surface is decreased (Tsutsumi et al., 1992). With progressive dealumination the electrostatic field inside the zeolite cages decreases and the surface becomes more hydrophobic. Therefore the strong polar attraction energies between the surface and molecule are reduced and weaker dispersion forces become dominant. On the other hand, on the aluminum rich zeolite the nature of the interactions between surface and adsorptive are always polar what

results in a steep slope of the isotherm at low partial pressures. Also with decreasing aluminum content the surface hydrophobicity increases and the adsorption equilibrium becomes more ideal and the zeolite surface becomes more homogeneous, so that real molecule-surface interactions are reduced (Sakuth et al., 1998).

4.1.3. Heat of adsorption

The surface properties of a solid are of primary importance in governing the energetics of the adsorption, reaction and desorption steps, which represent the core of a catalytic process. These properties can be conveniently investigated by studying the adsorption of suitably chosen probe molecules on the solid. Adsorption occurs at the interface between a fluid phase and a solid. The process is originated by the presence on the surface of coordinately unsaturated species able to interact with molecules from the gas phase, whose concentration at the interface results increased in comparison with that in the bulk gas phase. According to the relationship:

$$\Delta G_{\text{Ads}} = \Delta H_{\text{Ads}} - T \Delta S_{\text{Ads}} \quad (4.2)$$

where adsorption is generally exothermic, $\Delta H < 0$, as it occurs spontaneously ($\Delta G < 0$) and leads to a more ordered state ($\Delta S < 0$).

The heat evolved is called the heat of adsorption and can be determined in two ways: either by calculating the isosteric heats from adsorption isotherms, measured at two different temperatures, or by measuring the heat of adsorption directly with the aid of a calorimeter maintained at a chosen temperature (Auroux, 1997). Heat of adsorption is related to the energy of bonds formed and thus represents a measure of the strength of the interaction. In order to detect energetic heterogeneity of the surface, small doses of probe molecules have to be admitted successively on the solid, in order to saturate the active sites progressively. Recently, microcalorimetry has gained importance as one of the most reliable methods for the study of gas-solid interactions. Most commonly used are heat flow microcalorimeters of the Tian-Calvet type (Solinas et al., 1998).

4.2. Selectivity

Selectivity is the relative adsorption of components which is expressed as;

$$\text{Selectivity}_{1,2} = (x/y)_1 / (x/y)_2 \quad (4.3)$$

It is the ratio of the mole fractions in the pore divided by the mole fractions in the bulk. Selectivity in a physical adsorption system may depend on differences in either equilibrium or kinetics, but the great majority of adsorption separation processes depend on equilibrium based selectivity.

When selectivity values are greater than 1, it is much easier for the gases to be separated. Therefore the adsorbents should be chosen appropriately so that separations become easier (Clarkson et al., 1999).

For a given adsorbent, the relative strength of adsorption of different adsorbate molecules depends on the relative magnitudes of the polarizability α , dipole moment μ , and quadrupole moment Q of each. Often, just the consideration of the values of α , μ and Q allows accurate qualitative predictions to be made of the relative strengths of adsorption of given molecules on an adsorbent or of the best adsorbent type (polar or nonpolar) for a particular separation. For example, the strength of the electric field F and the field gradient of the highly polar cationic zeolites is strong. For this reason, nitrogen is more strongly adsorbed than is oxygen on such adsorbents, primarily because of the stronger quadrupole of N_2 compared to O_2 . In contrast, nonpolar activated carbon adsorbents lack strong electric fields and field gradients. Such adsorbents adsorb O_2 slightly more strongly than N_2 , because of the slightly higher polarizability of O_2 . Relative selectivities on nonpolar adsorbents often parallel to the relative volatilities of the same compounds. Compounds with higher boiling points are more strongly adsorbed. In this case the higher boiling O_2 is more strongly adsorbed than is N_2 .

For a given adsorbate molecule, the relative strength of adsorption on different adsorbents depends largely on the relative polarizability and electric field strengths of adsorbent surfaces. For example water molecules, with relatively low polarizability but a strong dipole and moderately strong quadrupole moment, are strongly adsorbed by polar adsorbents (eg. cationic zeolites), but only weakly adsorbed by nonpolar adsorbents (Ruthven D.M., 1984).

Besides, the size, dipole and/or quadrupole moments and polarizability of molecules often point to the most appropriate mechanism for the separation in polar zeolites, i.e. equilibrium, kinetic and steric. Equilibrium and kinetic separations are based upon the differences in capacity and diffusion rates, respectively, while steric separation results from the exclusion of one or more of the gases in the mixture from the zeolite pores (Ackley, 2002).

4.3. Selectivity Control

In zeolites, the specificity or selectivity shown toward particular adsorbate molecules may be modified by methods which alter energy of interaction terms. This can be done by adjusting the balance between electrostatic and Van der Waals forces.

Structural differences resulting from Si/Al ratio or from the method of dehydration and cation exchange can be utilized to exclude molecules from the zeolite framework, hinder diffusion, alter pore volume and change the adsorbate equilibrium capacity. The cation type, size, charge density, location and the extent to which it is exposed to the adsorbate molecules have a strong effect upon both adsorption capacity and selectivity. Clearly, modifications and the resulting induced structural/chemical changes greatly extend the gas separation potential of natural zeolites (Ackley, 2002).

The chemical nature of the surface and pore size can be changed by using the below stated methods:

- Preloading: By introducing small amounts of a polar adsorbate (such as water), which selectively locates on the most energetic sites and is adsorbed strongly enough that it may not be displaced by another less selective adsorbate molecule.
- Cation exchange: Affects the local electric field as well as adsorbate polarization.
- Decationization: Complete removal of the cations from the zeolite framework alters the local electric fields and field gradients and consequently reduces any interaction with a molecule with a permanent electric moment.
- Purification: By the removal of impurities from the adsorbent, the pores and the surface area of the natural zeolite are enlarged, hence this indeed does effect the selectivity (Breck, 1973).

4.4. Ideal Adsorbed Solution Theory (IAST)

IAST (Myers and Prausnitz, 1965) is an important method for the prediction of multicomponent gas adsorption, where the adsorbed phase is treated as ideal (Mathias et al., 1996). The IAS theory is a very popular and thermodynamically consistent predictive method.

It's necessary at the outset to have a specific system to which the IAST equations apply. This poses an immediate problem because the interfacial region is ill defined. This difficulty is circumvented by a trick devised by J. Willard Gibbs. The gas phase does not extend unchanged all the way to the solid surface. In the neighborhood of the solid, the gas phase properties change, but they do not change abruptly. There is a region of change, and although the gradients in the properties with distance from the surface may be large, they are not infinite. Therefore the extent of the interfacial region nor the exact distance into the gas phase that the solid makes its influence felt cannot be known. Therefore the real situation is replaced with a hypothetical one which is the gas phase persists unchanged up to the solid surface. Besides, the adsorbed phase is treated as a two dimensional phase with its own thermodynamic properties (Ness et al., 1969).

After Gibbs visualized the adsorbed phase as a two-dimensional film of condensed molecules on a solid surface, two dimensional, intensive variables (spreading pressure π and surface area A) have been introduced (Sakuth et.al., 1998). The spreading pressure may be pictured as the force acting between adsorbate molecules parallel to the surface. While there is no direct technique available for the measurement of the spreading pressure, it can be calculated from the change of other measurable properties (Talu et al., 1987). This idea allows applying the general concepts of phase equilibrium thermodynamics to adsorption equilibria (Sakuth et al., 1998).

When one uses the equilibrium criterion that the chemical potential in the adsorbed phase is equal to the chemical potential in the gas phase, the equation for mixed gas adsorption equilibrium at constant temperature is given by;

$$P y_i = P_i^o(\pi) \gamma_i \quad (4.4)$$

where γ is the activity coefficient, y_i the mole fraction of component i in the gas phase and x_i the mole fraction of the same component in the adsorbed phase. P is the total gas pressure and $P_i^0(\pi)$ is the equilibrium gas phase pressure corresponding to the solution temperature and solution spreading pressure for the adsorption of pure component i . In the case of ideal solution, the activity coefficient is equal to unity for all values of temperature (T), spreading pressure (π) and adsorbed phase mole fraction of component i (x_i). In this case equation (1) reduces to

$$Py_i = P_i^0(\pi)x_i \quad (4.5)$$

The theory assumes that the adsorbed phase is an ideal solution of the adsorbed components and the reduced spreading pressure (π^*) of all the components in the mixture in their standard states is equal to the reduced spreading pressure of the adsorbed mixture (π^*). Thus,

$$\pi_1^* = \pi_2^* = \pi_3^* = \pi_4^* = \dots = \pi_n^* = \pi^* \quad (4.6)$$

The reduced spreading pressure of each component is computed from Gibb's adsorption isotherm as follows;

$$\pi_i^* = \frac{\pi_i}{RT} = \int_0^{P_i^0} \frac{n_i}{P_i} dP_i \quad (4.7)$$

Where P_i^0 is the partial pressure of the single component i in its standard state. $n_i(P_i)$ is the adsorption isotherm, which in the present case is the Langmuir equation.

The total adsorbed amount of the gas n_T is calculated from x_i as follows:

$$\frac{1}{n_T} = \sum_{i=1}^N \frac{x_i}{n_i^0} \quad (4.8)$$

where n_i^0 is the amount adsorbed in the standard state calculated from an isotherm at the pressure P_i^0 . The actual amount of each component is, therefore,

$$n_i = n_T x_i \quad (4.9)$$

The above six equations provide the necessary framework for IAS mixed adsorbate predictions. The solution strategy is facilitated by first obtaining P_i^0 as an analytical function of π^* .

4.4.1. Solution Strategy

Step #	Action
1	1a. First the input parameters are supplied: the parameters for the single component isotherm, the total gaseous pressure and the mole fractions in the gas phase
2	<p>2a. the reduced spreading pressure as the molar average of the following integral is estimated</p> $z = \pi A / R_g T = \sum_{j=1}^N y_j \int_0^P \frac{C_{\mu j}}{P_j} dP_j$ <p>Total pressure is used as the upper limit of the integral</p> <p>2b. The RHS of the above equation can be evaluated because all variables (y,P, and the single component isotherm equations) are known. If the pure component isotherm can be approximated by a Langmuir equation, then the initial estimate of the spreading pressure can be taken as:</p> $z = C_{\mu s} \ln \left(1 + \sum_{i=1}^M b_i P_i \right)$ <p>where $C_{\mu s}$ can be taken as the average of the maximum adsorbed concentration of all species.</p>
3	3a. Knowing the estimated reduced spreading pressure from step 2, pure component pressure P_j^0 that gives that reduced pressure using the below equation is evaluated.

	$\frac{A\pi}{R_y T} = \int_0^{P_1^0} \frac{C_{\mu 1}}{P_1} dP_1 = \int_0^{P_2^0} \frac{C_{\mu 2}}{P_2} dP_2 = \dots = \int_0^{P_N^0} \frac{C_{\mu N}}{P_N} dP_N$ <p>then the amount adsorbed is evaluated for the single component from the single component isotherm at that hypothetical P_j^0</p> <p>3b. Next $F(z^{(k)})$ and $F'(z^{(k)})$ are calculated from the below equations</p> $F(z^{(k)}) = \sum_{j=1}^N \frac{Py_j}{P_j^0(z^{(k)})} - 1$ $F'(z^{(k)}) = \left[- \sum_{j=1}^N \frac{Py_j}{[P_j^0(z)]^2} \frac{dP_j^0(z)}{dz} \right]_{z=z^{(k)}} = \left[- \sum_{j=1}^N \frac{Py_j}{[P_j^0(z)] C_{\mu j}^0} \right]_{z=z^{(k)}}$ <p>and thence the reduced spreading pressure for the next iteration step can be calculated from the below equation.</p> $z^{(k+1)} = z^{(k)} - \frac{F(z^{(k)})}{F'(z^{(k)})}$
4	Step 3 is continued until the method converges.

Ideal adsorbed solution theory is being used by many authors in order to predict binary gas adsorption of gases from pure gas adsorption data and these are given in Table 4.1.

Table 4.1: Previous Studies Involving IAS Theory

Author and date	Gas pair	Adsorbent	Predictive model	Selectivity
Alan L. Myers et al (1973)	N ₂ /O ₂ CO ₂ /O ₂ CO ₂ /N ₂	5A and 10X molecular sieves	IAST	CO ₂ over O ₂ CO ₂ over N ₂
Orrin K. Crosser et al (1980)	CO ₂ /C ₃ H ₈ CO ₂ /C ₃ H ₆	5A molecular sieves	IAST	CO ₂ over C ₃ H ₈ CO ₂ over C ₃ H ₆
John T. Nolan et al (1981)	O ₂ /CO N ₂ /CO	10X molecular sieves		
Orhan Talu et al (1986)	CO ₂ /H ₂ S. C ₃ H ₈ /CO ₂ C ₃ H ₈ /H ₂ S	H-Mordenite	SPD IAST RAST	
Robert W Triebe et al 1995	CO/N ₂	Turkish Clinoptilolite	IAST VSM Extended Langmuir	CO over N ₂
Paul M. Mathias et al (1996)	N ₂ /O ₂	5A molecular sieves	IAST HIAST	N ₂ over O ₂
Orhan Talu et al (1996)	N ₂ /O ₂	5A zeolite	IAST	N ₂ over O ₂
M. Sakuth et al (1998)	Toluene/1-propanol	Y-zeolite	IAST PRAST	Toluene
C. Özgen Karacan et al (1999)	CO ₂ /CH ₄	Coal	IAST	CO ₂ over CH ₄
C.R. Clarkson et al (1999)	CO ₂ /CH ₄	Coal	IAST	CO ₂ over CH ₄
P. Kluson et al (2000)	CH ₄ /N ₂	Graphitic adsorbents	IAST	CH ₄ over N ₂
Salil U. Rege et al (2001)	CO ₂ /H ₂ O	NaX γ-alumina	Doong Yang IAST RAST	CO ₂ over H ₂ O
Shizhang Quiao et al (2002)	C ₂ H ₆ /C ₃ H ₈	Ajax activated carbon	MPSD-IAST MPSD-Ext.Lang	

As can be seen from Table 4.1, many scientists have been used IAST in order to predict binary gas adsorption.

CHAPTER 5

EXPERIMENTAL

5.1. Materials

In this study, the materials used as adsorbents were acid treated clinoptilolite-rich natural zeolite tuff and synthetic zeolites of 5A and 13X. The natural zeolite tuff obtained from Gördes-Fındıcak (Manisa, Turkey) region in 3 m depth from the surface was crushed and sieved to the particle size range of 850-2000 μ m. Then it was washed with distilled water for 2 hours at 60⁰C to remove the soluble salts. From XRD patterns shown in Figures 5.1 and 5.2 it was determined that the major phase of the washed zeolite (NCW) was clinoptilolite-heulandite with impurities such as quartz and cristoballite. The clinoptilolite-rich heulandite-clinoptilolite zeolites were treated with HCl, HNO₃ and H₂SO₄ to prepare the adsorbents. According to the chemical composition of the washed zeolite measured by using ICP is as follows; for wt % of oxides of Al₂O₃, SiO₂, MgO, Na₂O, K₂O, CaO, Fe₂O₃ and H₂O are 14.1, 64.2, 1.8, 1.7, 5.3, 1.0, 1.8 and 10.3 respectively.

The code of the adsorbents and their treatment time and temperature are presented in Table 5.1.

Table 5.1: Adsorbents used in the study

Zeolite Code	Definition	Treatment Time and Temperature
NCW	Natural zeolite tuff washed with distilled water	2 hours at 60 ⁰ C
C1-6h	Treated with 1 M HCl Solution	3 hours at 60 ⁰ C
C3-3h	Treated with 3 M HCl Solution	3 hours at 60 ⁰ C
C5-6h	Treated with 5 M HCl Solution	6 hours at 60 ⁰ C
P1	Treated with 1.1 M H ₃ PO ₄ Solution	6 hours at 60 ⁰ C
N2	Treated with 2 M HNO ₃ Solution	6 hours at 60 ⁰ C
5A	Synthetic zeolite-Aldrich (Lot # 04224HA)	No treatment was applied
13X	Synthetic zeolite-Aldrich (Lot # 04603BR)	No treatment was applied

Adsorption characteristics of the zeolites were obtained by using the N₂ adsorption at 77 K. The results are given in Table 5.2.

Table 5.2: Adsorption characteristics of the some of the adsorbents studied at 77K (Becer, 2003)

	NCW	C1-6h	C5-6h	C3-3h	N2	P1
V _{mic} ^a	0.005	0.029	0.063	0.056	0.068	0.04
A _{ext} ^a	3.08	6.2	25.8	17.2	22.5	6.5
n ^b	1.00	1.60	1.61	2.26	2.63	1.88
E ^b	11.05	19.31	21.63	20.98	25.42	25.23
V _{lim} /V _{max} ^c	0.77	0.9	0.87	0.89	0.86	0.86
r ^d	11.3	6.7	6.3	6.5	6.0	5.8
Si/Al	4.04	5.25	8.4	6.08	6.18	5.01

- a V_{mic}, micropore volume (cm³/g) and A_{ext}, external surface area (m²/g) calculated from t-plot
- b V_{lim}, limiting micropore volume (cm³/g), n, exponential constant, E, characteristic energy (kJ/mol) calculated from Dubinin-Astakhov (P/P₀=0,0001-0,1)
- c V_{max}, maximum amount adsorbed at relative pressure P/P₀ of 0,89
- d r^d, Hovarth-Kowazoe median pore diameter

As can be seen from Table 5.2, the Si/Al ratio was increased by the acid treatment. As a result of the acid treatment, not only the aluminum but also the charge-balancing cations were removed from the zeolite tuff. The removal of the aluminum and the cations decreased the energetic heterogeneity of the adsorbents (increasing “n” value). Besides, wide pore size distribution with low pore size diameter was obtained. In fact, the micropore structure of the zeolites was improved due to the increase of the accessible volume for N₂ and the external surface area, A_{ext}.

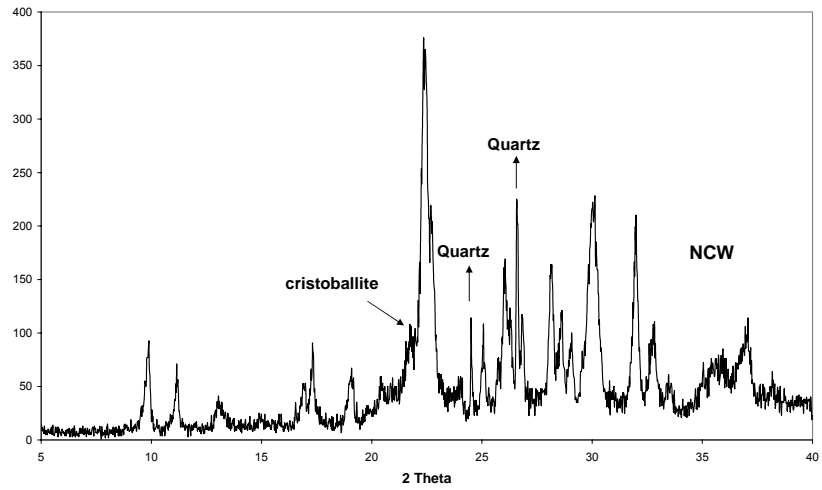
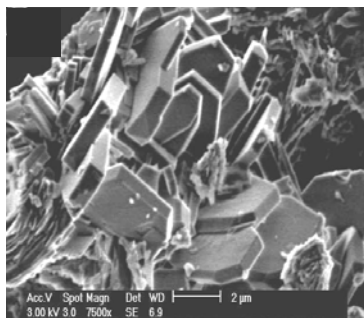
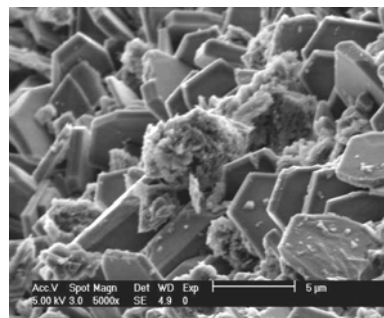


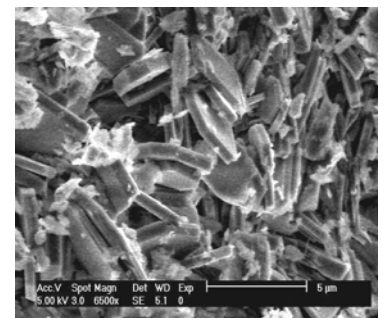
Figure 5.1. X-ray diffraction patterns of the washed natural zeolite (NCW)



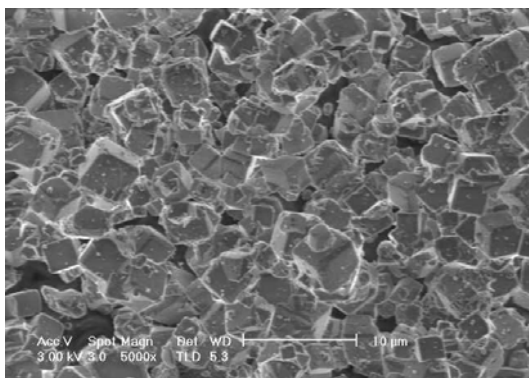
NCW



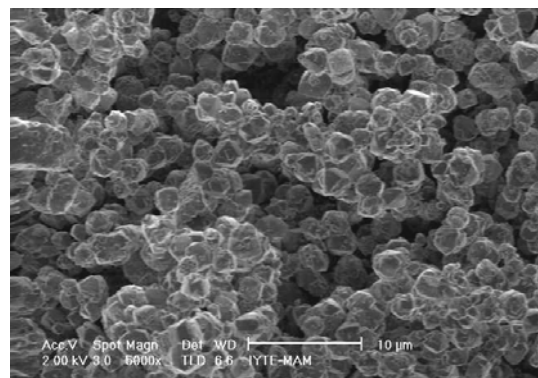
C3-3h



P1



5A zeolites



13X zeolites

Figure 5.2. SEM Micrographs of the zeolites

The SEM micrographs (Figure 5.2) clearly show that there are impurities present on the washed natural zeolite. The impurities are also detected by XRD analysis (Figure 5.1) and it was determined that impurities in the natural zeolite tuff were quartz and cristoballite.

When the SEM micrographs of 5A and 13X are compared, on a 10 μ m scale, the crystal size of 5A zeolites which are about 3.5 μ m are greater than that of 13X zeolites which are approximately 2 μ m (Figure 5.2).

Adsorbates

There are several parameters affecting the adsorption phenomenon, hence being reflected on the heat of adsorption in microcalorimetry studies. In fact, the size and the strength of the probe molecule and the temperature at which the adsorption takes place are important parameters and have to be carefully considered when performing adsorption studies.

In this study, CO₂, N₂ and Ar adsorbates were used. These molecules were chosen because they cover a fairly good range of molecular weights, molar volumes and polarizabilities. The properties of the adsorbate gases used in this study namely, CO₂, N₂ and Ar were given in Table 3.1. Also, the adsorption of these molecules provides a powerful tool for characterizing zeolites, by probing the cations and providing information on their nature and accessibility.

5.2. Methods

The adsorption isotherms of CO₂, N₂ and Ar gases on the acid treated natural and synthetic zeolites have been obtained through volumetric adsorption device. Furthermore, in order to be able to detect the surface heterogeneity of the adsorbents and the interaction taking place among the adsorbent-adsorbate gas pair, calorimetric studies were performed. Heat of adsorption values of CO₂, N₂ and Ar gases on the stated adsorbents were investigated.

5.2.1. Adsorption Studies

The Micromeritics (ASAP 2010) volumetric adsorption device was used to perform the adsorption experiments for N₂, Ar and CO₂ gases at 5°C and 25°C. In order to be able to keep the adsorption temperature constant, circulating water bath was used and all the tubing was covered with polymeric isolation material. Prior to

adsorption experiments, the zeolites were outgassed at 350°C for 24 hours under 5µmHg vacuum. The gases used in this study were highly pure (purity higher than 99%). CO₂ gas was further purified by using a three cartridge system filter to remove water, oxygen and hydrocarbons. With the use of two different temperatures, isosteric heats of adsorption of these gases have been calculated to be able to make comparison with the results obtained from microcalorimetry directly. Besides, the adsorption capacities of the acid modified natural zeolites as well as synthetic zeolites at two different temperatures towards CO₂, N₂ and Ar gases have been investigated. The adsorbents investigated are the acid modified zeolites ;C1-6h, C3-3h, C5-6h, N2 and P1 which have been treated with 1M HCl acid for six hours, 3M HCl acid for 3 hours, 5M HCl acid for 6 hours, 2M HNO₃ acid for 6 hours and 1.1M H₃PO₄ acid for 6 hours, respectively. The other investigated samples are washed natural zeolite (NCW), synthetic zeolites of 5A and 13X.

5.2.2. Calorimetric Studies

Microcalorimetry has gained importance as one of the most reliable methods for the study of gas-solid interactions. In order to determine the adsorption characteristics of the gases used in this study, the amount adsorbed by the adsorbent giving rise to heat evolution was required to be known. For this purpose, the most frequently used systems are Tian-Calvet type calorimeters. In this study, the heats of adsorption were measured at 298 K by a calorimeter of Tian-Calvet C80, Setaram in order to evaluate the enthalpy changes ($q^{diff} = -\Delta H_{ads}$) related to the adsorption. Before each experiment the zeolite was outgassed with a heating rate of 1°C/min and the temperature was ramped from 25 °C to 275 °C. Once 275 °C was reached, it was kept at this temperature for 5 hours. Afterwards, it was cooled down to room temperature with the same rate.

This calorimeter allowed differential heats of adsorption and standard gas isotherms to be collected so differential heats of adsorption could be plotted as a function of surface coverage. Gas adsorption microcalorimetry provided information regarding the change of the heat of adsorption with the surface coverage along with the total heat of adsorption and the total amount of gas adsorbed. Besides, the adsorption took place by repeatedly sending doses of gas onto the initially outgassed solid while recording the heat flow signal and the concomitant pressure evolution. The adsorption temperature was maintained at a constant value of 25 °C in order to

limit physisorption. The experiments were carried out isothermally by admitting stepwise increasing doses of the adsorbate gas to the zeolite previously evacuated. The initial dose sent to the system was 50 mbar. Since the initial doses were small enough, the heat obtained could be considered as a differential heat of adsorption. At each dose, the equilibrium pressure was added to the sending incremental dose (50 mbar). Afterwards, the dose amount was increased to 300 mbar and the procedure was repeated until no further pressure drop was observed. The heat evolved by each dose was measured and the corresponding amount adsorbed was obtained by the pressure drop in the known volume of the apparatus. This was determined in previous calibration by allowing a known amount of gas to expand from the measure section into the vessels section formerly evacuated. For each dose, thermal equilibrium was attained before the pressure p_i , the adsorbed amount δn_{ads} and the integral heat evolved δQ^{int} were measured. The adsorption experiments were concluded when a relatively high pressure was reached without the significant evolution of heat and the adsorbed amount became negligible.

In order to determine the differential heat of adsorption from the data obtained by microcalorimetry, the measured enthalpy was divided by the quantity of adsorbed molecules for each dose. The heat was determined by integrating the calorimetric data, and the quantity of adsorbed molecules was calculated using the collected pressure data. Amounts adsorbed were expressed as mmol/g of zeolite outgassed at 275 °C.

The calorimetric data were reported here as differential heats, $q^{\text{diff}} = \delta Q^{\text{int}}/\delta n_{\text{ads}}$. Hence the differential heat of adsorption is defined as the enthalpy change in going from the gas phase to the adsorbed phase.

Microcalorimetry employs two cells namely reference cell which is empty and the zeolite cell which contains the zeolite to be tested.

A step-wise procedure was followed in this study. In Figure 5.3, the components of the microcalorimetry system are shown which are; the pressure control panel, electric shalter, microcalorimetry and CS32 device required transferring data. At the inset, a small picture of the pressure control panel is shown with the valves numbered from 1 to 4 from left to right respectively. The valve just above the pressure control panel is named as valve 5.



Figure 5.3: Photograph of the Microcalorimetry System

First of all valve 5 was closed to isolate the microcalorimetry from the rest of the set up. Then gas regulation was made by opening valve 4 and the gas was trapped within valves 4 and 5. After the gas was trapped, valve 4 was closed and the gas taken was sent to the system by opening valve 5. A pressure drop was observed which was determined by pressure transducer due to adsorption process in the sample cell of the microcalorimetry. It was waited until heat flow value reached its minimum. Then valve 5 was closed and the procedure was repeated for the next step. The dosing apparatus was connected to a computer which controlled the temperature of the heated box, indicated the heat flow values as peaks with respect to time. In all experiments degas temperature ($275\text{ }^{\circ}\text{C}$) and sample mass ($\sim 0.50\text{g}$) were kept constant. The first dose sent to the system was 50 mbar. After equilibrium is reached, equilibrium pressure is added to 50 mbar for the next step. Afterwards, dose pressure was increased to 300 mbar until no further adsorption takes place in the sample cell.

CHAPTER 6

RESULTS AND DISCUSSION

6.1. Adsorption Studies

Equilibrium isotherm data of CO₂ and N₂ on the zeolites were obtained at 5 °C and 25 °C. Langmuir and Sips model equations were applied to the data in order to determine the heterogeneity parameters considering the correlation coefficients. Henry's constants were obtained by using the Virial adsorption equation to calculate the pure component selectivity. Also, energy distribution curves are presented to analyze the heterogeneity of the adsorbents.

6.1.1. Adsorption Isotherms

The CO₂ and N₂ adsorption isotherms are presented in Figures 6.1 and 6.2, respectively. It can be seen from Figure 6.1 that the CO₂ adsorption isotherms of the zeolites are of type 1 which have nearly rectangular shapes. In these zeolites, there is an abrupt increase of adsorption at low equilibrium pressures. It's known that the amount of cations which represent the active specific centers for the adsorption of CO₂ molecules depends on the Si/Al ratio (Hernandez et al., 1999). Uptake of CO₂ on the acid treated forms of zeolites changed with the Si/Al ratio. The slight decrease in CO₂ adsorption was observed for the acid treated zeolites depending on the dealumination degree, Si/Al ratio, which are higher than the Si/Al ratio of NCW (4.04).

From Figure 6.1, it's seen that the zeolite which adsorbs CO₂ the most are synthetic zeolites namely 5A and 13X. It is also determined that CO₂ is adsorbed comparatively by P1 and NCW zeolites. Because Si/Al ratio of the P1 and NCW zeolites are close to each other which are 5.01 and 4.04 respectively. In order to determine the temperature effect on the adsorption capacity of the zeolites, experiments were carried at 5 °C and 25 °C. Fresh zeolites were used for the experiments performed at both temperatures. Because the used samples gave lower CO₂ adsorptions on the same samples (Figure 6.1). This means that the adsorbed CO₂ molecules couldn't be removed properly during outgassing at 350 °C for 24 hours. As

the temperature increased the adsorbed amount decreased since adsorption is an exothermic process.

In Figure 6.2, it's clearly seen that among the acid treated natural zeolites the N₂ adsorption is the highest in P1 sample for both temperatures. On the other hand, 5A synthetic zeolite has the highest adsorption capacity for N₂. When the temperature effect on adsorption is investigated, the adsorption capacity of the N2 sample is influenced the most by the temperature difference as can be seen in Figure 6.2. As it is expected, as temperature increases, the adsorbed amount decreases. C1-6h and C3-3h samples are affected the least by the temperature difference.

Additionally, it is observed that adsorbed amount of N₂ on synthetic zeolites change linearly with the equilibrium pressure, while for natural zeolites and its modified forms, the shape of the isotherms exhibit a shape closer to the rectangular isotherm.

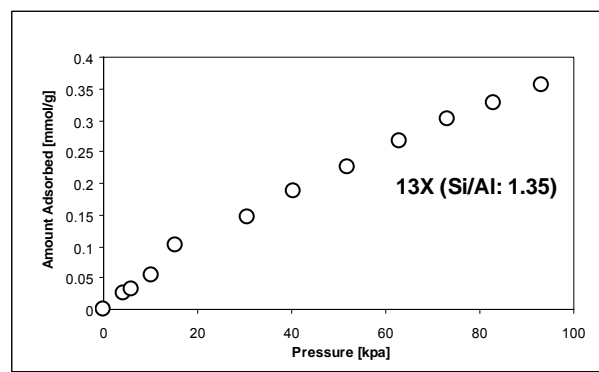
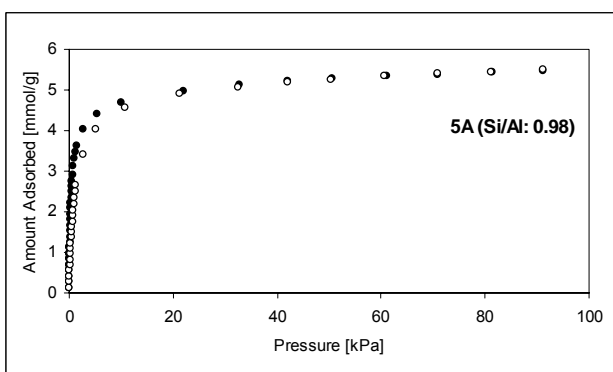
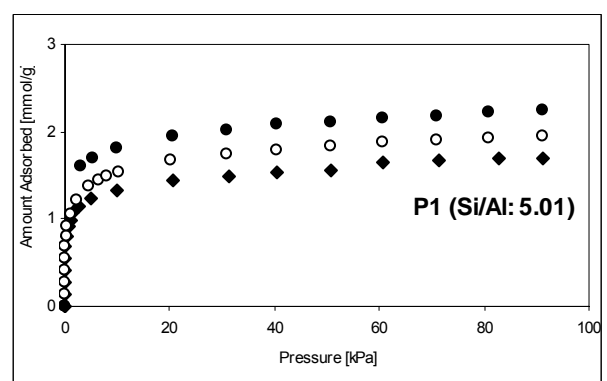
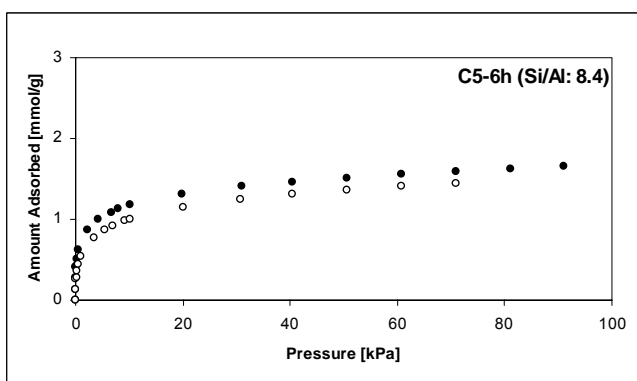
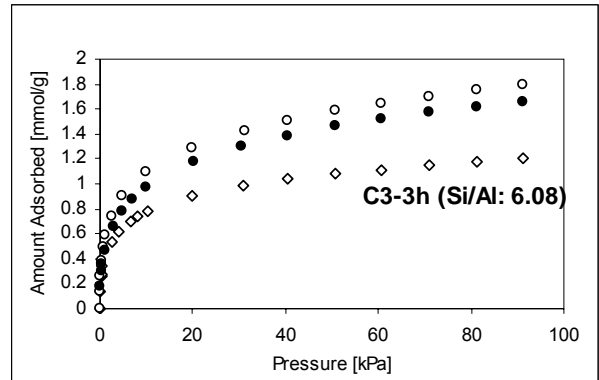
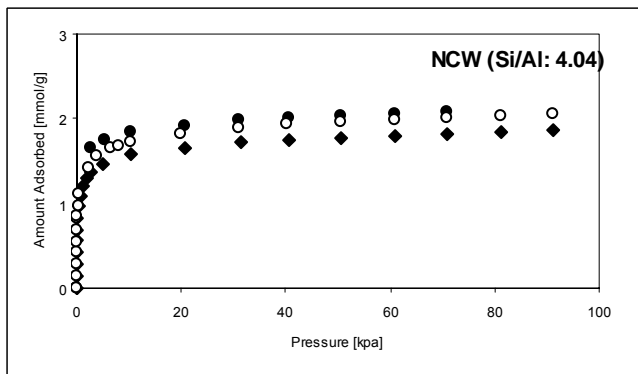


Figure 6.1: CO₂ Adsorption Isotherms on the used and fresh Adsorbents at 5 °C (●); 25 °C (○) (◆); used sample at 5 °C.

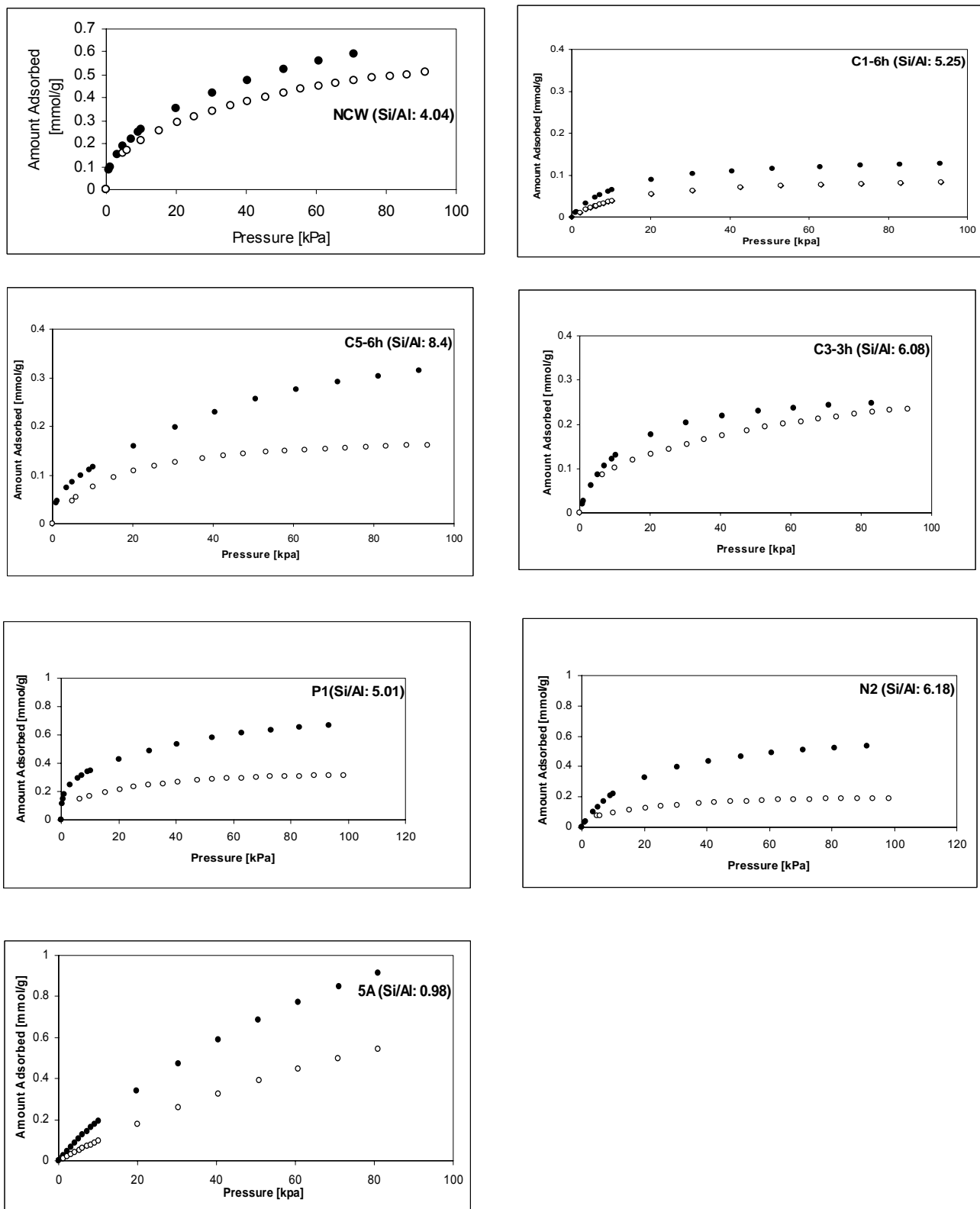


Figure 6.2: N_2 Adsorption Isotherms on the zeolites at 5 °C (●); 25 °C (○).

6.1.2. Adsorption Capacities of the Zeolites for CO₂ and N₂ Adsorption

From the CO₂ and N₂ adsorption data, the maximum adsorption capacities of zeolites were obtained and presented in Tables 6.1 and 6.2.

Table 6.1: Maximum adsorption capacities of zeolites for CO₂ Adsorption

Zeolites	Temperature [°C]	Pressure [kpa]	Maximum Adsorbed Amount [mmol/g]
5A	5	91	5.46
	25		5.48
13X	5	91	-
	25		6.82
NCW	5	91	2.084
	25		2.05
C3-3h	5	93	1.79
	25		1.66
C5-6h	5	91	1.658
	25		1.44
P1	5	93	2.24
	25		1.95

In CO₂ adsorption, the highest adsorption capacity belongs to synthetic zeolites. This can be explained due to lower Si/Al ratios of these zeolites. Among the natural zeolites, NCW has the highest adsorption capacity. It's not treated with acid and therefore has the lowest Si/Al ratio. Consequently, the lower the Si/Al ratio, the higher the specific interactions are. Due to higher specific interactions between the CO₂ and zeolite the adsorbed CO₂ by the zeolite resulted in high value. The adsorption capacity of the NCW and P1 samples are similar to each other due to being closer Si/Al ratios which are 4.04 and 5.01 for NCW and P1, respectively.

Table 6.2: Maximum adsorption capacities of zeolites for N₂ Adsorption

Zeolites	Temperature [°C]	Pressure [kpa]	Maximum Adsorbed Amount [mmol/g]
5A	5	81	0.91
	25		0,58
13X	5	91	-
	25		0.31
C1-6h	5	93	0.13
	25		0.07
C3-3h	5	93	0.26
	25		0,23
C5-6h	5	91	0.31
	25		0.16
P1-6h	5	93	0.67
	25		0.31
N2-6h	5	91	0.54
	25		0.19
NCW	5	91	0.59
	25		0.51

N₂ adsorption capacities of the zeolites at both temperatures are compared in Table 6.2. The capacities were determined at about 90 kPa. 5A zeolite gives the highest adsorption capacity while C1-6h zeolite has the lowest adsorption capacity. However, the orders are changed with respect to temperature which are as follows; 5A > P1 > N₂ > 13X ~ C5-6h > C3-3h > C1-6h at 5 °C and 5A > 13X > P1 > C2-3h > N₂ > C5-6h > C1-6h at 25 °C. From the order, it can be concluded that 5A synthetic zeolite has the highest adsorption capacity and among the acid modified natural zeolites P1 zeolite has the highest adsorption capacity. P1 also has the highest monolayer capacity among the acid modified natural zeolites. It is expected that as the specific interactions with the gas molecules are high, more molecules are adsorbed by the P1 sample.

Table 6.3: Previous Studies of N₂ and CO₂ Adsorption on Zeolites

Zeolites	Amount adsorbed (mmol/g)	Pressure (kPa)	Adsorbate	T(°C)	Author
clinoptilolite	0.59	101.3	N ₂	22	Rege S.U. et al., 2000
clinoptilolite	2.5	20.26	CO ₂	22	
clinoptilolite	1.83	20	CO ₂	25	This study
clinoptilolite	0.65	91.2	N ₂	27	Ackley M.W. et al.,1991
Clinoptilolite	0.32	27	N ₂	27	Hernandez et al., 1999
Clinoptilolite	1.7	27	CO ₂	17	
clinoptilolite	0.4	100	N ₂	30	Triebe R.W. et al.,1995
13X	0.44	101.3	N ₂	22	Rege S.U. et al., 2000
13X	6	35.5	CO ₂	22	
13X	6	80	CO ₂	31.4	Ustinov E. et al., 1999
13X	6.82	90	CO ₂	25	This study
13X	0.48	101.3	N ₂	22	Jayaraman A. et al.,2002
5A	0.6	100	N ₂	23	Talu O. et al., 1996
5A	0.58	90	N ₂	25	This study
5A	0.27	90	N ₂	20	Warmuzinski et al., 1999
5A	2.548	80	CO ₂	30	Pakseresht S. et al.,2002
5A	5.48	90	CO ₂	25	This study

The adsorption capacities of the zeolites for CO₂ and N₂ used in this study are compared to the literature data in Table 6.3. The CO₂ adsorption on natural zeolite at 20 kPa is determined as about 1.83 mmol/g at 25 °C in this study while Rege S. U. et al. (2000), found this value as 2.5 mmol/g at 22 °C. The reason for the small difference between the adsorbed amounts may be due to the temperature increase. Hernandez et al (1999) found the lowest adsorbed amount of CO₂, 1.7 mmol/g, at a lower temperature (17 °C) because of the impurities that the clinoptilolite has. Furthermore, in the studies performed by Ustinov et al. (1999), the amount of CO₂ adsorbed on 13X at 30 °C was determined as 6 mmol/g at about 80 kpa which is close to the value obtained in this study which is 6.82 mmol/g at 25 °C. When the adsorbed amount of 5A is compared with the literature data, the adsorbed amounts of CO₂ and N₂ on 5A in this study at 25 °C are greater than the adsorbed amount in the studies of Pakseresht S. et al. (2002) and Warmuzinski K. et al. (1999). They have found that 5A zeolite adsorbs 2.548 mmol/g of CO₂ and 0.27 mmol/g of N₂ at 30 °C and 20 °C respectively while in this study, at around 90 kpa, the adsorbed amount of CO₂ and

N₂ are 5.48 and 0.58 mmol/g respectively. Talu et al. (1996) also reported that N₂ adsorbed amount on 5A at 23 °C was 0.6 mmol/g and in this study it was found as 0.58 mmol/g at 25 °C.

6.1.3. Model Equations

Different model equations were applied to the adsorption data obtained from volumetric studies in order to get information regarding the heterogeneity of the adsorbent surfaces. The models applied to the data are Sips, Dubinin Astakhov, Langmuir equations and also Henry's constants from Virial plot are presented. By making use of the data obtained from the heterogeneity parameters of the applied equations, interpretation of the results is made.

Langmuir Model Equation

Langmuir model is applied to adsorption data for CO₂ and N₂ at 5 °C and 25 °C. The Langmuir parameters of the zeolites for CO₂ and N₂ are given in Tables 6.4 and 6.5, respectively.

Table 6.4: Langmuir Parameters of Some Zeolites for CO₂ Adsorption

Adsorption Temperature (°C)		NCW	C3-3h	C5-6h	P1	5A	13X
5 °C	b	5.09	0.33	1.15	0.72	1.98	-
	n _m [mmol/g]	1.68	1.65	1.46	2.18	5.19	-
	Correlation Coeff. [%]	96.55	98.17	95.83	99.39	99.59	-
25 °C	b	6.64	0.20	0.56	2.44	0.76	0.41
	n _m [mmol/g]	1.84	1.62	1.32	1.74	5.36	6.46
	Correlation Coeff. [%]	96.53	98.39	97.27	96.54	99.83	98.77

Parameter b in Langmuir Model is called the affinity constant. It is a measure of how strong an adsorbate molecule is attracted onto a surface. When the affinity constant b is larger, adsorbate-adsorbent pair is more heterogeneous. The highest b parameter for CO₂ adsorption is obtained for NCW sample, and P1 sample follows the NCW at both temperatures. This is expected because Si/Al ratios and the X-ray diffraction patterns of these two zeolites are close and, therefore yield similar affinity towards CO₂. The SEM micrographs of P1 and NCW also show that the zeolites still

have crystalline structure after acid treatment (Figure 5.1). Therefore, the undamaged crystalline structure did not have a negative effect on adsorption capacity of these zeolites.

Table 6.5: Langmuir Parameters of the samples for N₂ Adsorption

Adsorption Temperature (°C)		NCW	C1-6h	C3-3h	C5-6h	P1	N2	5A	13X
5 °C	b	0.067	0.082	0.084	0.045	0.130	0.050	0.011	0.007
	n_m [mmol/g]	0.67	0.14	0.28	0.37	0.67	0.65	1.95	0.72
	Correlation Coeff. [%]	99.13	97.92	98.33	99.17	97.60	99.38	99.99	99.98
	Si/Al ratio	4.04	5.25	6.08	8.4	5.01	6.18	0.98	1.35
25 °C	b	0.05	0.082	0.046	0.068	0.086	0.082	0.006	0.006
	n_m [mmol/g]	0.598	0.087	0.28	0.19	0.35	0.21	1.58	1.01
	Correlation Coeff. [%]	99.28	99.38	98.73	99.47	99.19	99.11	99.99	99.84

It is seen from Table 6.5 that P1 sample has the highest b parameter at both temperatures, which are 0.13 and 0.09 for 5°C and 25°C respectively. This indicates that it is more heterogeneous when compared to the other adsorbents. It also has relatively lower correlation coefficient at 5°C. Besides, as temperature increases, the b values decrease for NCW, P1, C3-3h and 13X zeolites.

For N₂ adsorption, correlation coefficients of Langmuir Model are higher than those for CO₂ adsorption at both temperatures. The correlation coefficient of more than 98 and 95 % were obtained for N₂ and CO₂ respectively. The Langmuir model has represented the experimental data quite good for N₂ adsorption on the zeolites as shown in Figure 6.4.

Not only the adsorption isotherms but also the heterogeneity parameters of the synthetic zeolites 5A and 13X are presented, it can be said that there is a better fit of the experimental data with the Langmuir model for synthetic zeolites at 5°C and 25°C and their b parameter values are lower when compared to the other samples as shown in Table 6.5. As a result the affinity is higher for adsorbent-CO₂ gas pair, because the specific interactions between them are stronger than for adsorbent-N₂ gas pair.

Sips Model Equation

Another model applied to represent the experimental data is the Sips model. The experimental adsorption isotherms and the corresponding Sips Model are presented in Figures 6.3 and 6.4.

The correlation coefficients of the Sips Model are generally higher than 99 %. Their corresponding adsorption isotherms and the deviation of the model isotherms from the experimental data are shown in Figures 6.3 and 6.4.

The parameter t of the Sips Model characterizes the system heterogeneity and the larger is this parameter the more heterogeneous is the system. According to Table 6.6, P1 has the highest t value indicating that CO₂-P1 pair is more heterogeneous when compared to other adsorbent-gas pairs.

t parameters are lower for the synthetic zeolites so their b values in Sips and Langmuir models are close to each other.

Table 6.6: Sips Parameters of the Zeolites for CO₂ Adsorption

Adsorption Temperature (°C)		C3-3h	C5-6h	P1	NCW	5A	13X
5 °C	correlation coefficient[%]	99.99	99.99	99.99	99.92	99.89	-
	n_m (mmole/g)	3.22	2.64	5.37	2.03	5.40	-
	b (kpa ⁻¹)	0.019	0.050	0.001	2.25	1.67	-
	t (-)	2.48	3.07	6.52	2.41	1.29	-
25 °C	correlation coefficient[%]	99.97	99.99	99.69	99.85	99.96	99.97
	n_m (mmole/g)	1.04	2.38	2.4	2.30	5.60	9.65
	b (kpa ⁻¹)	0.0007	0.042	0.50	1.77	0.62	0.067
	t (-)	2.19	2.63	2.9	2.58	1.23	2.02

In a study performed by Pakseresth et al in 2002, the Langmuir and Sips Models were applied to the experimental data obtained from volumetric apparatus for CO₂ on 5A zeolite at 30 °C and they determined the n_m value of the Langmuir Model as 3.92 mmol/g and the t parameter of the Sips Model as 1.79 at these conditions. In this study for CO₂ adsorption on 5A at 25 °C these parameters were determined for n_m and b as 5.36 mmol/g and 1.23 respectively.

In the study performed by Hernandez et al. in 1999, the t parameter of the Sips Model applied to the CO₂ adsorption data of clinoptilolite at 27 °C was determined as 1.13 while in this study its determined as 2.58 for NCW at 25 °C .

Table 6.7: Sips Parameters of the Zeolites for N₂ Adsorption

Adsorption Temperature (°C)		NCW	C1-6h	C3-3h	C5-6h	P1	N2	5A	13X
5 °C	correlation coefficient[%]	99.99	99.93	99.87	99.87	99.97	99.82	99.99	99.86
	n _m (mmole/g)	8.21	5.17	1.25	8.05	3.56	8.33	2.26	9.13
	b (kpa ⁻¹)	4.9E-5	5.3E-7	5.7E-4	2.07E-5	1.5E-4	3.6E-5	8.13E-3	1.5E-4
	t (-)	2.22	2.76	2.33	1.99	2.94	2.19	1.05	1.25
25 °C	correlation coefficient[%]	99.99	99.43	99.98	98.36	99.95	99.81	99.99	99.86
	n _m (mmole/g)	1.40	0.097	0.98	3.21	0.43	0.26	1.62	1.58
	b (kpa ⁻¹)	0.0038	0.065	8.9E-4	1.67E-6	0.0498	4.6E-2	6.23E-3	2.74E-3
	t (-)	1.92	1.017	2.17	3.02	1.55	1.47	1.0	1.10

Adsorption isotherms of N₂ and CO₂ also show that, the consistency of the Sips Model with the experimental data are better than in Langmuir Model (Figures 6.3 and 6.4). In Table 6.7, it's determined that P1 has the highest heterogeneity for gases at 5 °C since it has the highest t values which are 3.18 and 2.94 kPa⁻¹ for CO₂ and N₂ respectively. When the t values are compared at both temperatures, it can be determined that at 5 °C, gas-adsorbent system is more heterogeneous since the t values are generally greater at 5 °C. Besides, CO₂-adsorbent system heterogeneity is greater than N₂- adsorbent system since the t values are greater in CO₂ adsorption. In case of N₂ adsorption on synthetic zeolites for both temperatures the t values are nearly 1, which indicate that synthetic zeolite-N₂ gas systems are more homogeneous. In this case, the correlated b values from Langmuir and Sips models are in good agreement with each other.

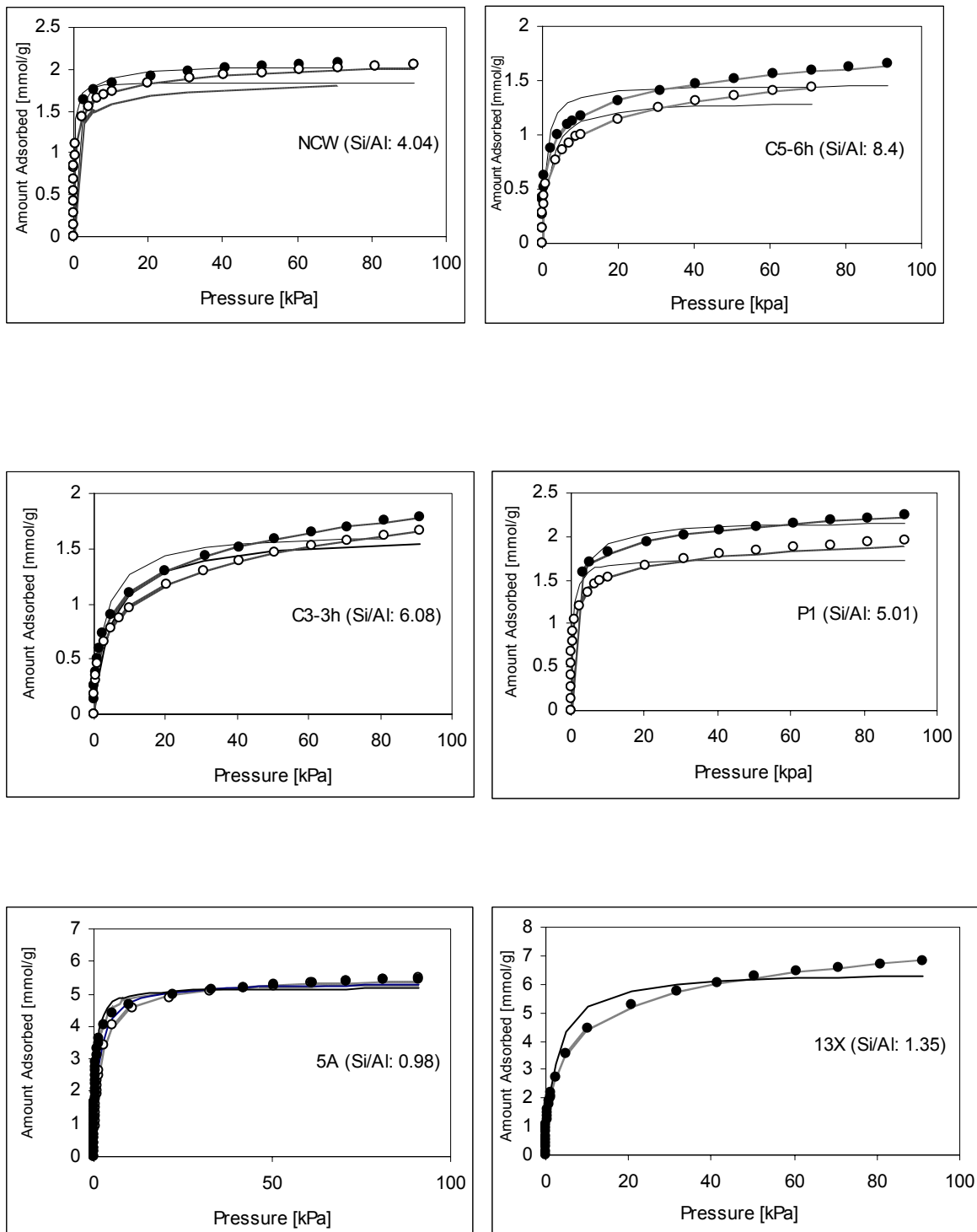


Figure 6.3: CO₂ Adsorption Isotherms on the zeolites at 5 °C (●); 25 °C (○).
 Points: experimental data, lines: Langmuir Model, dashed lines: Sips Model

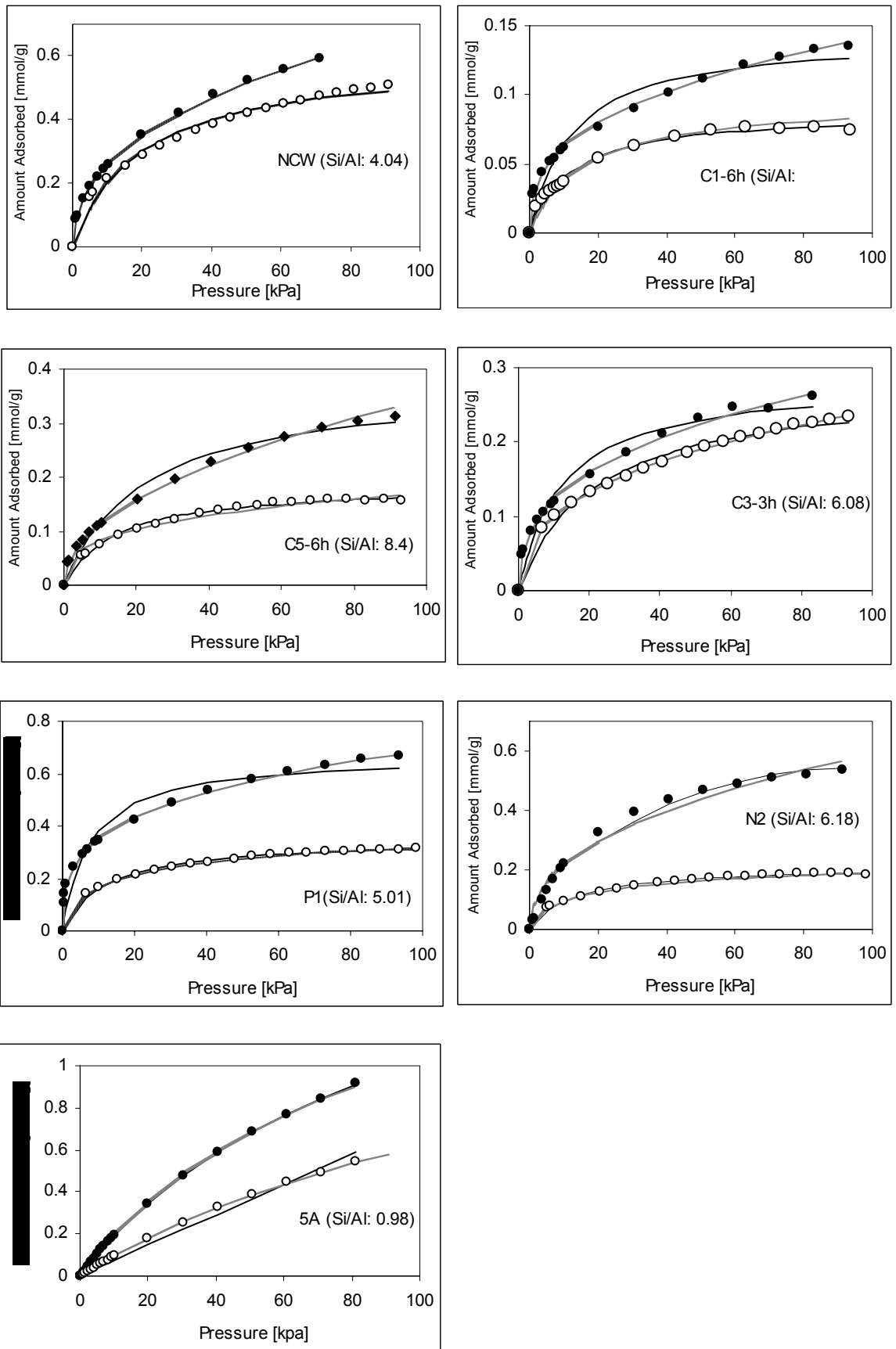


Figure 6.4: N₂ Adsorption Isotherms on the zeolites at 5 °C (●); 25 °C (○).
 Points: experimental data, lines: Langmuir Model, dashed lines: Sips Model

Selectivity

Pure component selectivity can be calculated by using the Henry's constant obtained from the pure component adsorption data. The Virial equation in the linear form;

$$\ln\left(\frac{n}{P}\right) = K_1 + K_2n + K_3n^2 + \dots \quad (6.1)$$

was used to calculate Henry's constant, k_H , which is related to K_1 , the interaction parameter between the adsorbent and gas molecules. They are presented for CO_2 and N_2 in Table 6.8.

$$k_H = \lim_{p \rightarrow 0} (n/p) \quad (6.2)$$

Table 6.8: Henry's Constants for the CO_2 and N_2 Adsorption

Sample	T [C ⁰]	k_H [mmol ⁻¹ kpa ⁻¹] for CO_2	k_H [mmol ⁻¹ kpa ⁻¹] for N_2
5A	5	10.39	0.021
	25	4.08	0.03
13X	5	-	-
	25	2.62	0.006
C1-6h	5	-	0.012
	25	-	0.007
C3-3h	5	0.54	0.024
	25	0.32	0.013
C5-6h	5	1.67	0.017
	25	0.73	0.013
P1	5	4.95	0.087
	25	4.54	0.03
N2	5	-	0.033
	25	-	0.017
NCW	5	8.59	0.045
	25	12.24	0.03

According to the Henry's constants given in Table 6.8, the interaction with CO_2 is the highest for P1 while it's the lowest for C3-3h at 5°C. In N_2 adsorption, the highest interaction parameter belongs to P1 zeolite and NCW follows it while the lowest interaction parameter was determined for 13X at 25 °C. Generally, Henry constants are higher for natural zeolites than synthetic zeolites. This indicates that the natural zeolites are rather energetically heterogeneous. Besides, as temperature

increases from 5 °C to 25 °C Henry's constants generally decrease which indicate that the interactions decrease as temperature increases.

Table 6.9: Selectivity Ratios of CO₂ over N₂ for the Adsorbents

Sample	T [C°]	Pure Component Selectivity Ratios (CO ₂ /N ₂)	Si/Al Ratio
5A	5	494	0.98
	25	136	
13X	5	-	1.35
	25	451	
C3-3h	5	22.5	6.08
	25	24.6	
C5-6h	5	98.2	8.4
	25	56.2	
P1	5	56.9	5.01
	25	151.3	
NCW	5	191	4.04
	25	408	

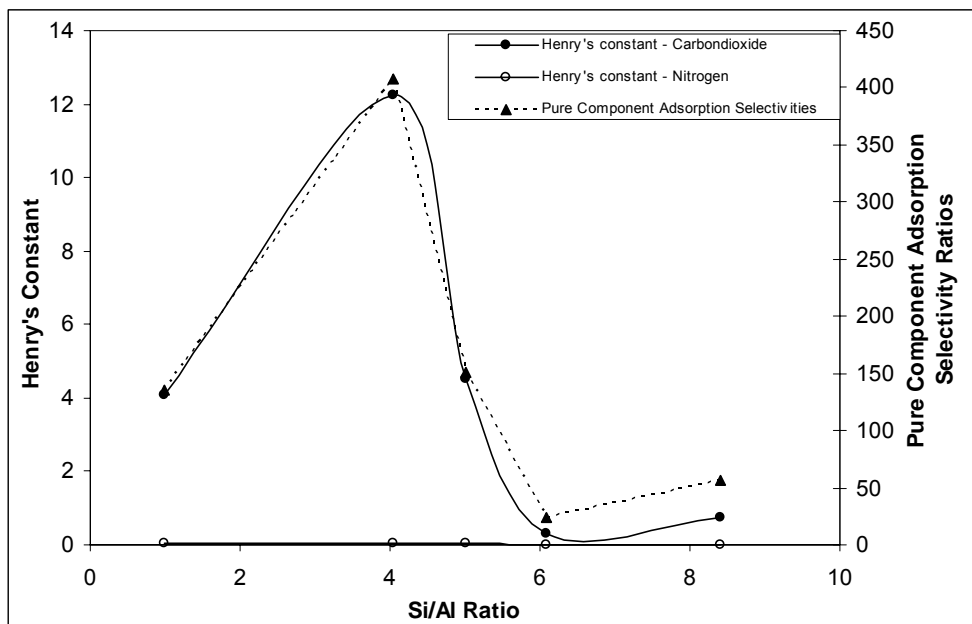


Figure 6.5: Change of Henry's Constants and Selectivity Ratios with Si/Al at 25 °C

Pure component selectivity ratios of CO₂ over N₂ are shown in Table 6.9. According to that, generally when the Si/Al ratio is around 4, the selectivity of CO₂ over N₂ is the greatest. Furthermore, Si/Al ratio has a significant effect on the change of Henry's constants for CO₂ due to the quadrupole moments of CO₂ gas however Henry constants for N₂ were not affected much by the change of Si/Al ratio.

6.1.4. Evaluation of the Energy Distributions

Rozwadowski et al. (1989) have reported that heterogeneity of the microporous adsorbents is connected closely with the distribution of adsorption potential in micropores. These distributions characterize the energetic heterogeneity of microporous solids and can be related to microporous structure (Gil et al., 1996). In this study, equation 6.3 has been used for the construction of energy distributions by taking the Dubinin Astakhov Equation as the basis.

$$X(A) = -dW / dA = -W_0(d\theta / dA) = (nW_0kA^{n-1} / \beta^n) \exp(-k(A/\beta)^n) \quad (6.3)$$

where A is the energy of adsorption in Dubinin Astakhov Equation, k and β are the structural parameters correlated with the micropore dimensions.

The potential energy distribution diagrams obtained from equation 6.3 are presented in Figures 6.6 and 6.7 for CO_2 and N_2 respectively.

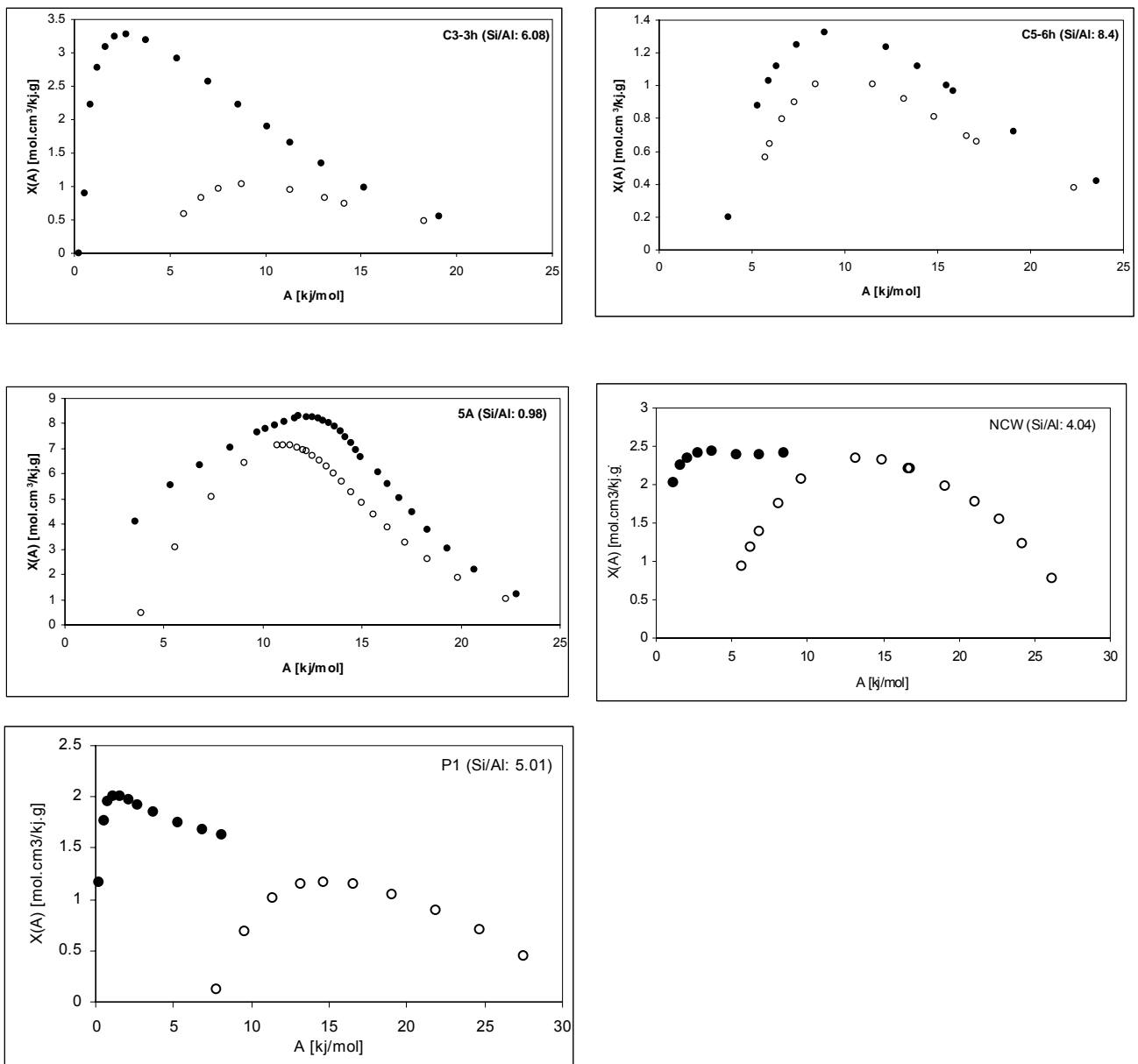


Figure 6.6: Adsorption Potential Distributions for CO₂ Adsorption at 5 °C (●); 25 °C (○).

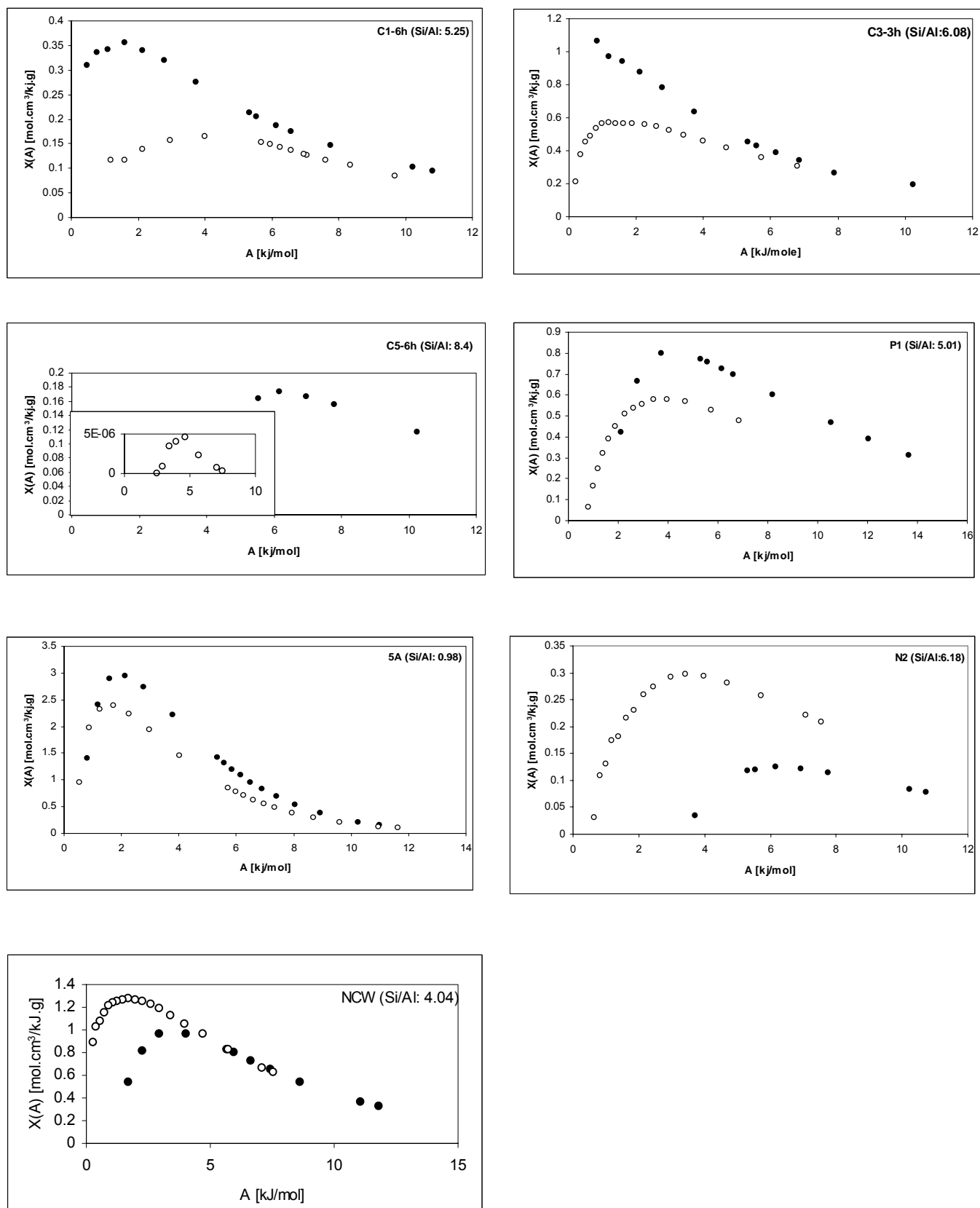


Figure 6.7: Adsorption Potential Distributions for N₂ Adsorption at 5 °C (●); 25 °C (○).

The energy distributions of CO₂ and N₂ are compared in Figures 6.6 and 6.7, it's seen that the spread of the energy distributions for CO₂ is in a wider range than for N₂. Gil et al. (1996), suggests that the larger A values are related to micropores of small size which in turn indicates higher heat of adsorption values. Therefore, the distributions indicate that CO₂-adsorbent system exhibits a more heterogeneous behavior than N₂-adsorbent system. As indicated previously, the specific interactions between CO₂ and the zeolites are greater than that of N₂. As can be seen from Figure 6.6, the energetic heterogeneity expressed by the energy distributions in increasing order is C5-6h < P1~NCW < C3-3h < 5A which is similar to the order of the adsorbents in terms of their adsorption capacities for CO₂ adsorption which is related to the heterogeneity of the adsorbent-adsorbate system for natural zeolites. Furthermore, when the effect of temperature is investigated, it's determined that system is more heterogeneous at 5°C as also proved by the shape of their adsorption isotherms.

In Figure 6.7, the energy distributions for N₂ adsorption are given. Similarly, gas-adsorbent systems generally have a wider energy distribution at 5°C. Especially, P1 zeolite has the highest heterogeneity in N₂ adsorption as also proved by calorimetric studies.

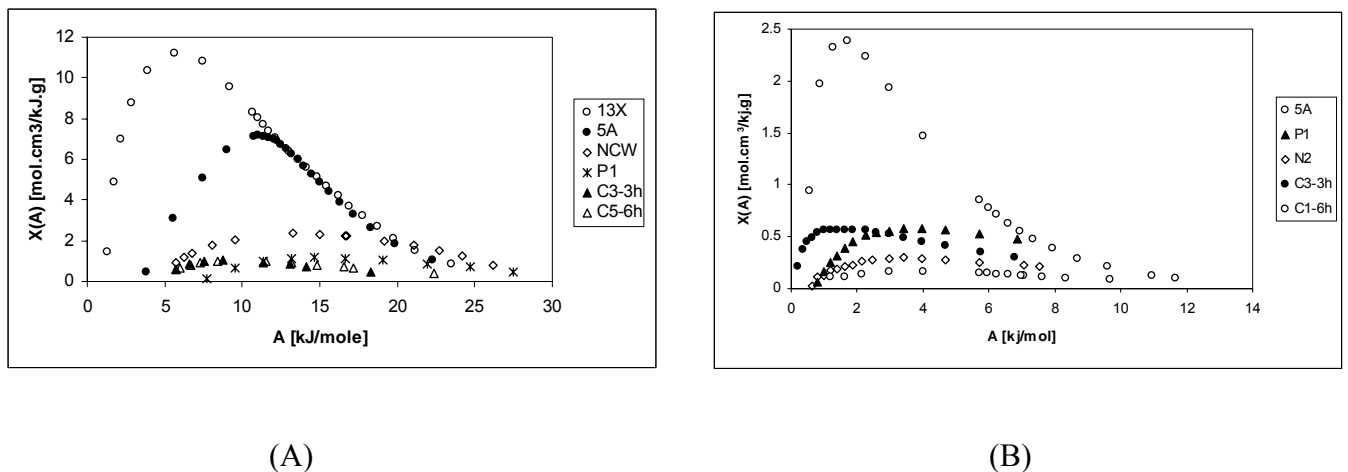


Figure 6.8: Adsorption Potential Distributions for (A) CO₂, (B) N₂ Adsorptions at 25 °C.

In Figures 6.8 A and B, adsorption potential distributions of the zeolites for CO₂ and N₂ at 25°C are given. According to these, synthetic zeolites have the widest energy distributions for both gases. C5-6h zeolite has the lowest potential energy

values for CO₂ while for N₂ C1 has the lowest among the other zeolites. Calorimetric results also support that the synthetic zeolites have higher heat of adsorption values and hence more heterogeneous while C1-6h and C5-6h have lower heat of adsorption values due to their higher Si/Al ratio.

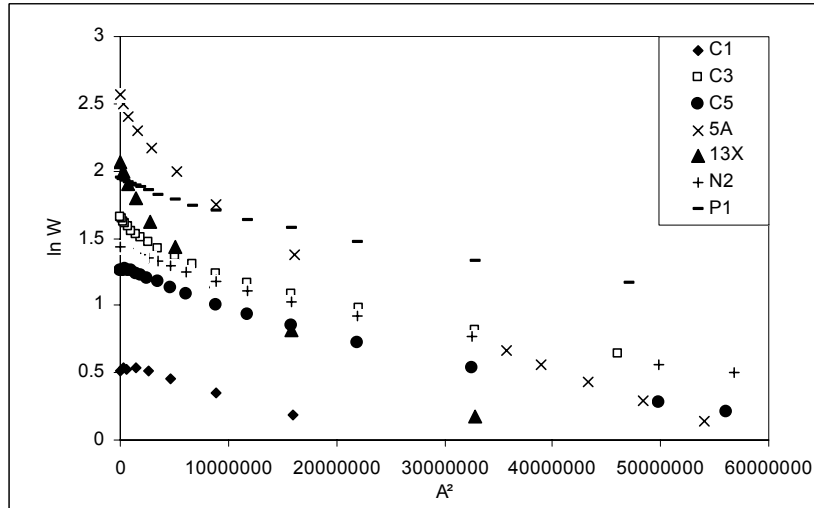


Figure 6.9: Characteristic Energies of the Zeolites for N₂ at 25°C

As can be seen from Figure 6.9, the lowest characteristic energy belongs to C1-6h zeolite while the highest one belongs to P1 zeolite among the acid treated natural zeolites. The order of the characteristic energies is consistent with the microcalorimetric data in which 5A zeolite has the highest heat of adsorption value which is about 103 kJ/mole while C1-6h has the lowest heat of adsorption which is about 38 kJ/mole.

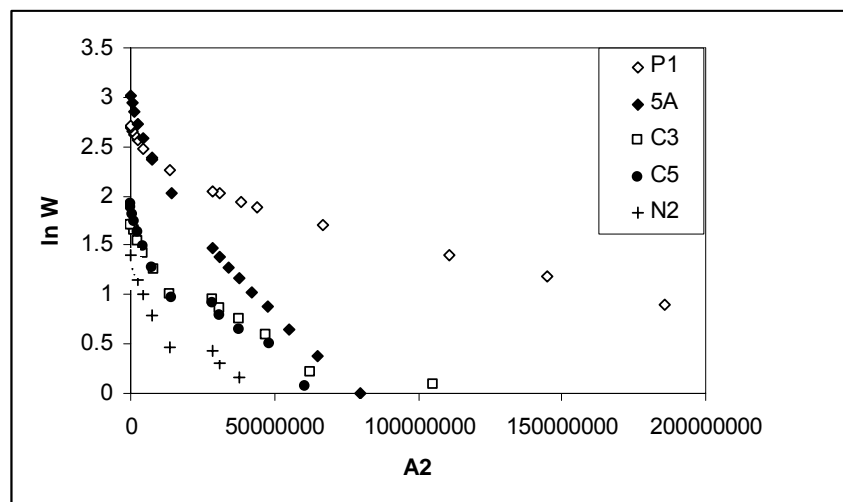


Figure 6.10: Characteristic Energies of the Zeolites for N₂ at 5°C

As can be seen from Figure 6.10, the adsorption potentials for the zeolites are greater at 5 °C. At this temperature also P1 sample has the highest characteristic energy among the acid treated natural zeolites.

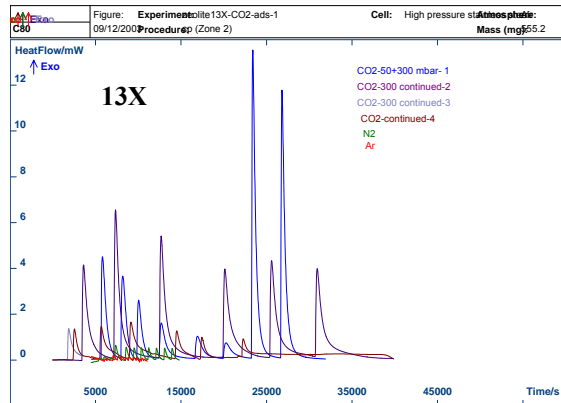
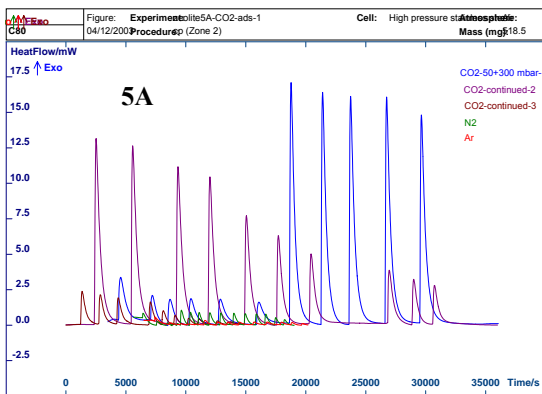
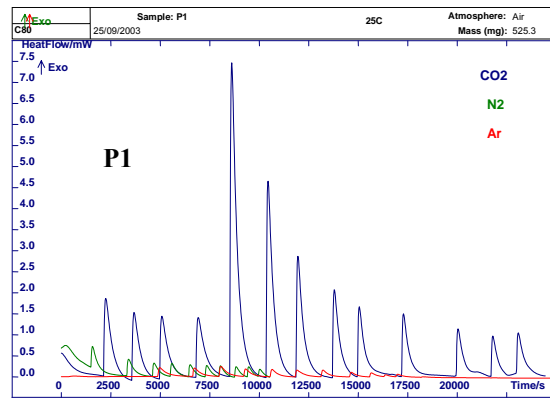
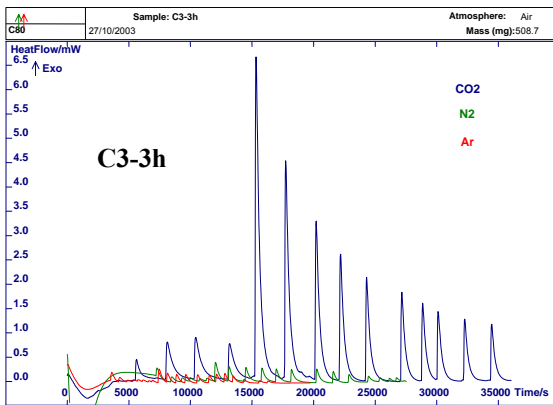
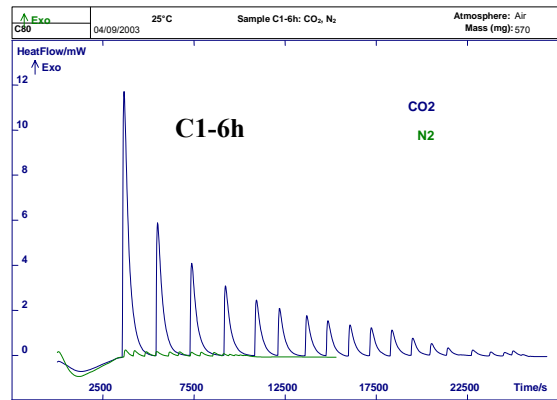
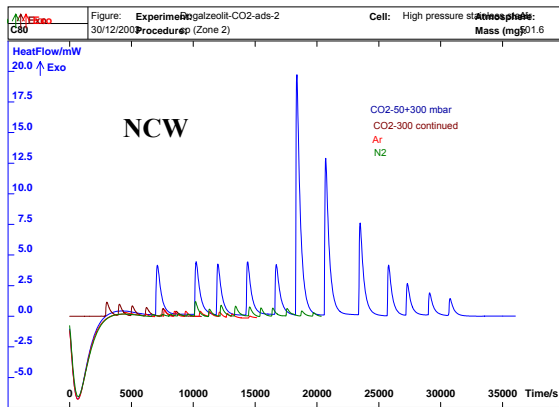
6.2. Calorimetric Studies

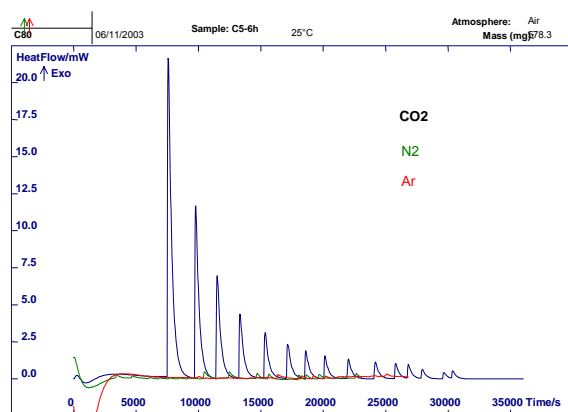
In calorimetric studies, differential heats of adsorption and adsorption isotherms have been measured simultaneously in a calorimeter for different gases (CO₂, N₂ and Ar) on a series of adsorbents such as acid modified natural zeolites and synthetic zeolites.

From the calorimetric studies, the calorimetric peaks and the change in the heat flow (mW) with respect to time were obtained. The calorimetric peaks were obtained by sending 50 mbars of dose intervals and then increased to 300 mbar until no further adsorption takes place in the zeolite cell.

In the investigation of the calorimetric curves, there are some important factors that have to be considered. The shape of a calorimetric curve appears to be strongly dependent on 3-dimensional differences in the molecular homogeneity of the framework structure. Most of the calorimetric profiles of differential heat of adsorption versus coverage show four regions: (i) an initial region of high adsorption heats, often ascribed to extraframework Lewis species, (ii) a region of intermediate strength sites, which is ascribed to Bronsted acid sites. In zeolites, there is always a pretty good relationship between the framework aluminum content and the population of Bronsted acid sites, provided that the framework aluminum atoms are totally accessible to the probe. A region of constant heat in this domain is characteristic of a set of Bronsted acid sites of homogeneous strength. (iii) a region where heats decrease more or less steeply depending on the heterogeneity of the sites and (iv) low heats of adsorption at high coverages, approaching a nearly constant value characteristic of reversible adsorption (Auroux, 2002).

6.2.1. Calorimetric Peaks of CO₂, N₂ and Ar on Zeolites





C5-6h

Figure 6.11: A set of calorimetric peaks obtained for CO₂, N₂ and Ar adsorptions on the zeolites (C1-6h: 300 mbar dose intervals, others 50 and 300 mbar dose intervals)

The calorimetric peaks of CO₂, N₂ and Ar on the zeolites under investigation are given in Figure 6.11. The initial low intensity peaks represent 50 mbar dose intervals while the latter high intensity peaks represent the 300 mbar dose intervals. The intensity of the peaks gradually decreases until no further adsorption takes place. As a result of this no further heat is evolved. The CO₂ peaks are the highest peaks whereas the lowest peaks belong to Ar gas. The intensity of the calorimetric peaks are higher for NCW and synthetic zeolites for CO₂. This shows that these adsorbents are energetically more heterogeneous and the specific interactions between these zeolites and CO₂ are greater. Figures also indicate that the CO₂ adsorption on the zeolites are the most energetic, while Ar adsorption is the least energetic as expected. The trend of decreasing the peak intensities as adsorption proceeds is similar in all the zeolite samples.

The values of q_{diff} (heat of adsorption) were calculated by using the area under each peak. In Figure 6.12, differential heat of adsorption graphs and their corresponding adsorption isotherms at the inset are given for CO₂. As can be seen from the figures, the heat evolved decreases with increasing the amount adsorbed. . The differential heats of adsorption extrapolated to zero coverage on zeolites, representing the enthalpy change for the adsorption on the most energetic sites active in the early stage of the process were determined from the curves and presented in the Table 6.10 at zero coverage, the heat of adsorption of CO₂ on NCW is around 80 kJ/mole.

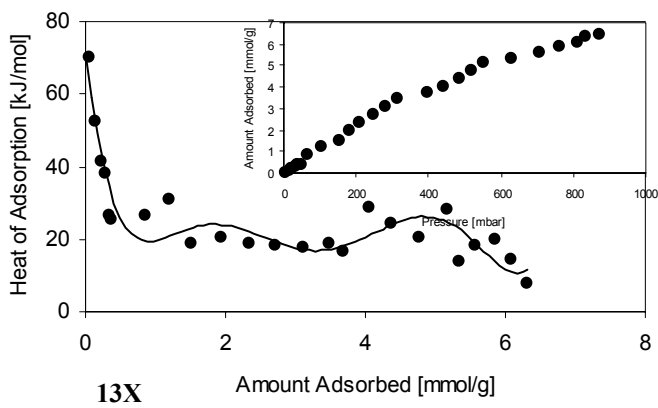
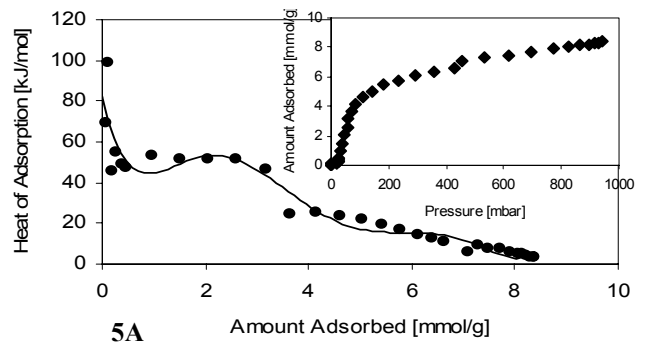
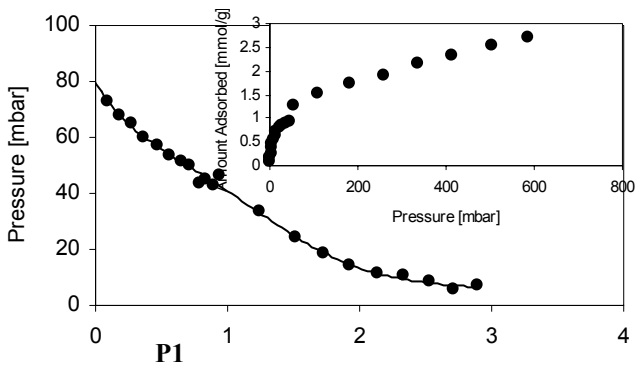
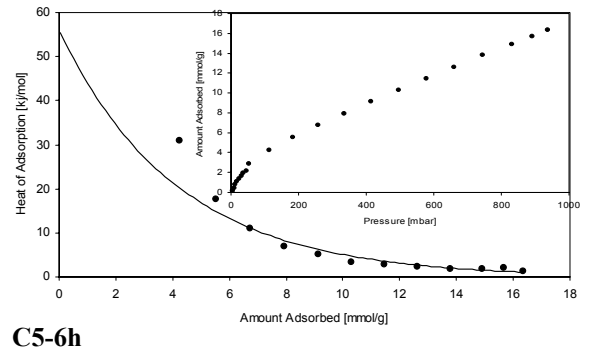
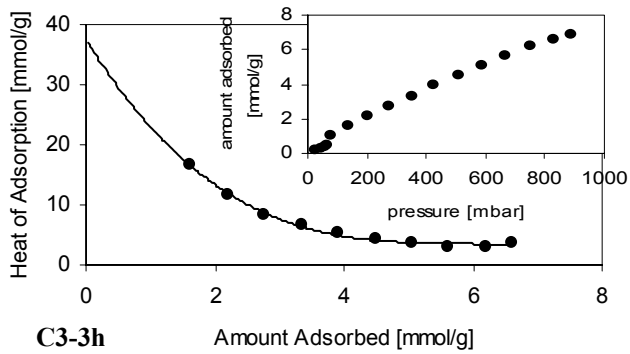
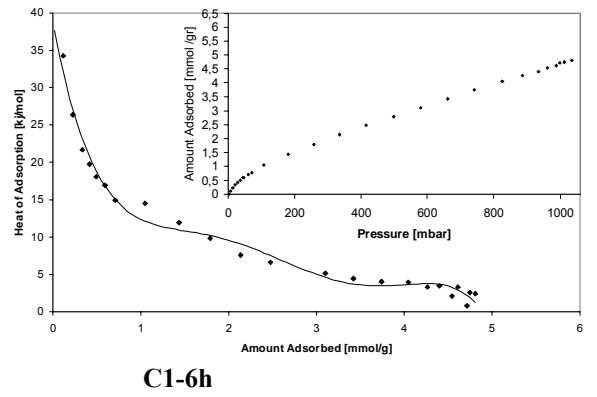
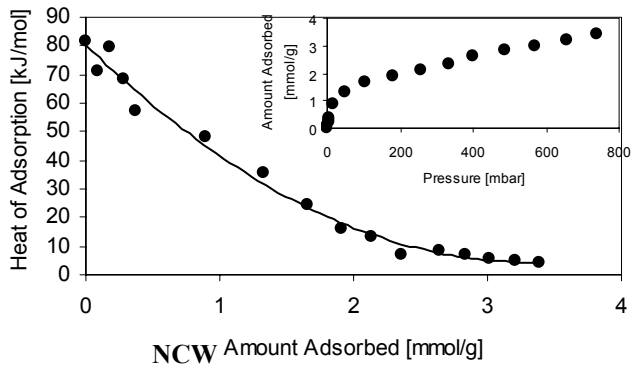


Figure 6.12: Differential Heat of Adsorption of CO₂ on Zeolites

NCW is the washed natural zeolite and has not been treated with any acid. Therefore it may be used as a reference adsorbent to make a comparison between the other adsorbents. Since *NCW* has not been treated with acid, it is expected that its surface is heterogeneous because aluminum cations and other cations responsible for creating polarity present in the zeolite structure have not been removed and the Si/Al ratio is 4.04 for *NCW* which is the lowest value among all of the natural zeolites.

The differential heat of CO₂ adsorption at zero coverage on ***C1-6h*** was determined as 38.54 kJ/mole which is lower than *NCW*. Differential heat of adsorption then rapidly decreases to about 5.16 kJ/mole as amount adsorbed increases that can be due to surface heterogeneity inside the micropores. Once these sites are saturated, a plateau is reached at around 3.42 kJ/mole that corresponds to the filling of the remaining micropores. This plateau also indicates the homogeneous sites forming a family of constant q_{diff} . At the end of this plateau, the decrease of the heat to 2.42 kJ/mole indicates the completion of the micropore filling.

Auroux (1997) states that, the way in which the heat of adsorption falls with increasing coverage varies both with the adsorbate and with the adsorbent. Besides, Solinas et al. (1998) states that, a continuous decrease of adsorption heat points out to the presence on the zeolite of strong sites not belonging to a same family.

The differential heat of CO₂ adsorption at zero coverage on the ***C3-6h*** zeolite with a Si/Al ratio of 6.08 is 37.52 kJ/mole (Table 6.10) . Then this value decreases to about 2.95 kJ/mol and then remains constant. When its corresponding adsorption isotherm is investigated, the maximum amount adsorbed was determined to be 6.9 mmol/g at a pressure of 892 mbar.

In CO₂ adsorption on *C5-6h* zeolite, the differential heat of adsorption of *C5-6h* at zero coverage is determined as 55.944 kJ/mole which decreases sharply to about 1.29 kJ/mole due to surface heterogeneity (Figure 6.12). The greater degree of dealumination increases the strong Bronsted sites so that the specific interactions between the adsorbent surface and the gas molecules are high due to higher Si/Al ratio. As it's reported in the literature, the cation density which is an important parameter in adsorption studies is controlled by dealumination which generally leads to a higher degree of energetic uniformity (Sing, 1999). However, the shape of the curve still indicates that there is extensive amount of heterogeneity on the surface of the zeolite. As the dealumination level is increased, the external surface area is

increased accordingly. Therefore, the adsorption capacity of the C5-6h zeolite is determined to be 16.34 mmol/g at a pressure of 937.5 mbar.

As in the HCl treated and NCW zeolites, the heat of CO₂ adsorption on the zeolite treated with H₃PO₄ decreases with increase in the amount adsorbed. The Si/Al, the degree of dealumination is the lowest for **P1** zeolite among the acid treated zeolites which is 5.01 and therefore the specific interaction between the CO₂ gas and the adsorbent surface is the greatest. The heat of adsorption of CO₂ on P1 at zero coverage is determined as 79.5 kJ/mole (Table 6.10). This high value of adsorption heat can indicate that strong interactions may result from the low Si/Al ratio and the phosphorous present on the surface of the zeolite with the CO₂ gas having a high quadrupole moment. The cations present in the P1 zeolite is determined by SEM-EDX analysis and according to that 0.293 wt % of phosphorous is present on the zeolite.

Differential heat of adsorption of CO₂ on **5A** at zero coverage is determined as 83.08 kJ/mole which is the highest heat of adsorption among the adsorbents. The heat of adsorption curve makes a minimum at about 14.16 kJ/mole then increases to about 53 kJ/mole due to adsorbate-adsorbate interactions.

The heat of adsorption of CO₂ on **13X** at zero coverage is around 72.75 kJ/mole. As a synthetic zeolite, 13X has high specific interactions with the CO₂ as in 5A zeolite due to its lower Si/Al ratio. Furthermore, the fluctuations in the heat of adsorption curves of 13X and 5A are due to adsorbate-adsorbate interactions.

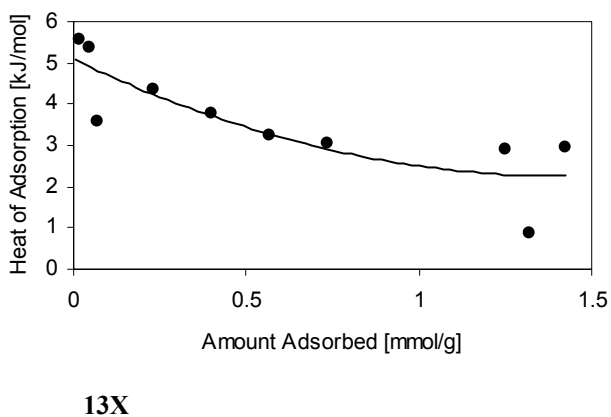
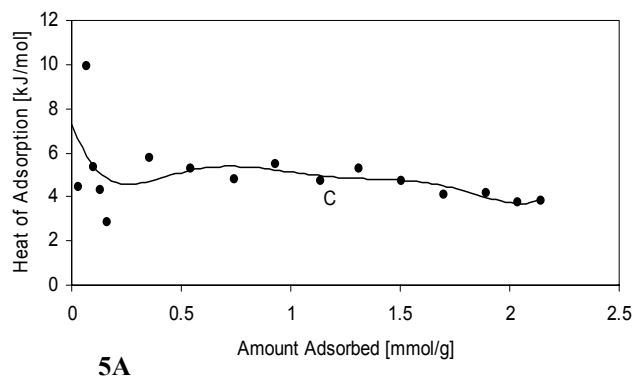
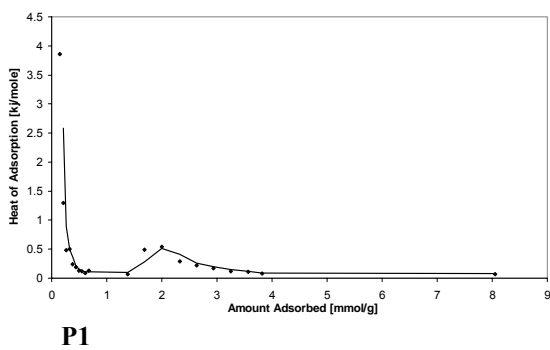
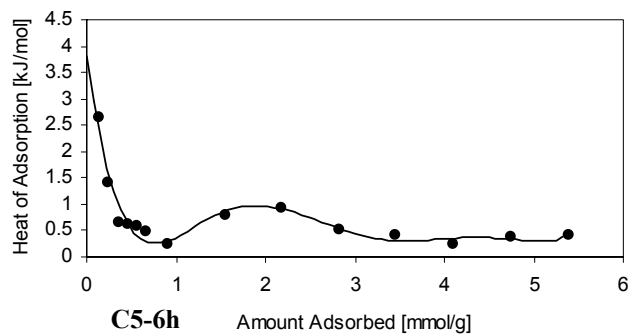
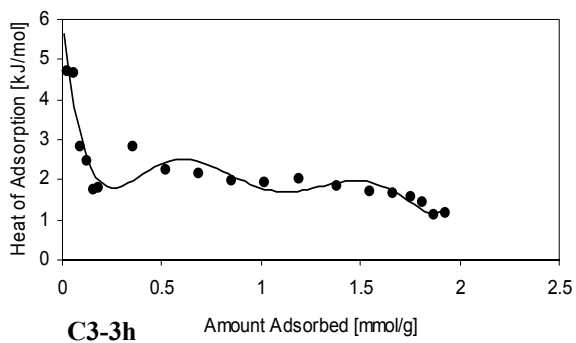
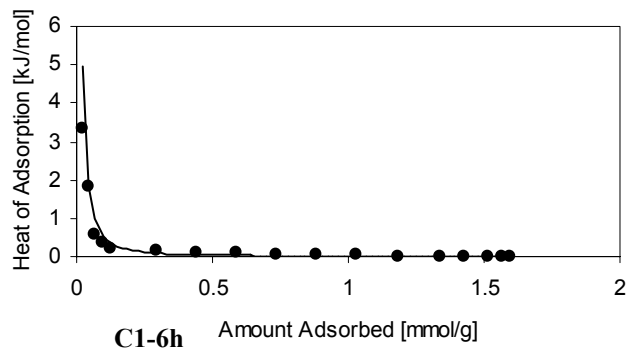
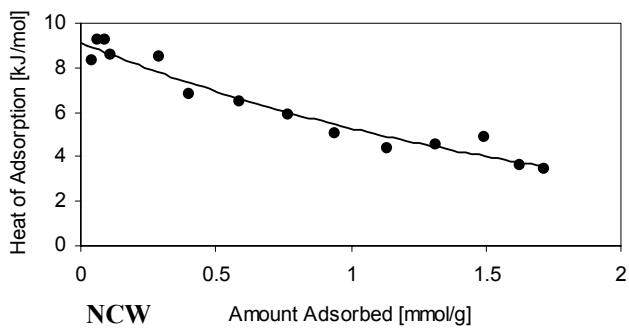


Figure 6.13: Differential Heat of Adsorption of N_2 on Zeolites

Figure 6.13 presents the differential heat of adsorption graphs of the zeolites for N₂ adsorption. The differential heat of adsorption values for N₂ adsorption are lower than CO₂ adsorption for all the samples. This can be explained due to the higher polarizabilities and the quadrupole moments of CO₂ gas which are 26.5x10⁻²⁵cc and 4.30x10⁻²⁶esu-cm² respectively. Consequently, the amount of adsorbed CO₂ and the adsorption heats are greater than that of N₂.

At zero coverage, the heat of adsorption value of N₂ on *NCW* is around 9.1 kJ/mole which is the highest adsorption heat value for N₂ adsorption among the acid treated natural zeolites due to the lowest Si/Al ratio of the *NCW* zeolite. As can be seen from Figure 6.13, there is a sharp decrease in differential heat of adsorption of N₂ on *C1-6h*. This indicates the existence of active sites of similar strength in the structure. This type of curve also shows that there is continuous heterogeneity at any coverage (Solinas et al., 1998).

Figure 6.13 also shows the differential heat of adsorption of N₂ molecule on the *C3-3h* zeolite. It can be seen that the differential heat of adsorption of this molecule at zero coverage is determined as 5.9671 kJ /mole with the maximum adsorbed amount of 1.928 mmol/g at 993.3 mbar. The value of differential heat of adsorption evolved as a result of first N₂ dose can be comprehended as a measure of the strength of the strongest active sites in the structure (Rakic, 2001). Again there is the maximum value of 5.9671 of differential heat at which the N₂ molecule interacts with the most active sites of the zeolite structure where it decreases to 1.81 kJ/mole.

The differential heat of N₂ adsorption is determined as 3.9192 kJ/mole at zero coverage for *C5-6h* with the maximum amount adsorbed 5.394 mmol/g at a pressure of 713.4 mbar (Figure 6.13). Then the value decreases to about 0.26 kJ/mole at which the most active sites of the zeolite surface is filled. Afterwards, the heat of adsorption value makes a maximum at about 0.45 kJ/mole at a loading of 4 mmol/g where probably the adsorbate-adsorbate interactions take place. Finally, the value remains constant at about 0.384 kJ/mole.

At zero coverage the heat of adsorption of N₂ on *PI* zeolite is 8.8577 kJ/mol and the maximum amount adsorbed is 1.61 mmol/g at a pressure of 876.9 mbar. The shape of the heat of adsorption curve is more or less similar to the other zeolites but the adsorption heat is greater than the others as expected. For *5A* synthetic zeolite heat of adsorption value of N₂ at zero coverage is 7.3 kJ/mole and gradually decreases to 3.77 kJ/mole and finally for *I3X*, again the heat of adsorption value at zero

coverage of N₂ on 13X is much lower than that of CO₂ which is 5.20 kJ/mol. The curve has a decreasing trend and then reaches a plateau at around 3 kJ/mole.

The fluctuation of the heat of adsorption values with coverage is a clear indication that there are active sites of different strength on the surface and as surface coverage increases, after completion of monolayer coverage, adsorbate- adsorbate interactions take place.

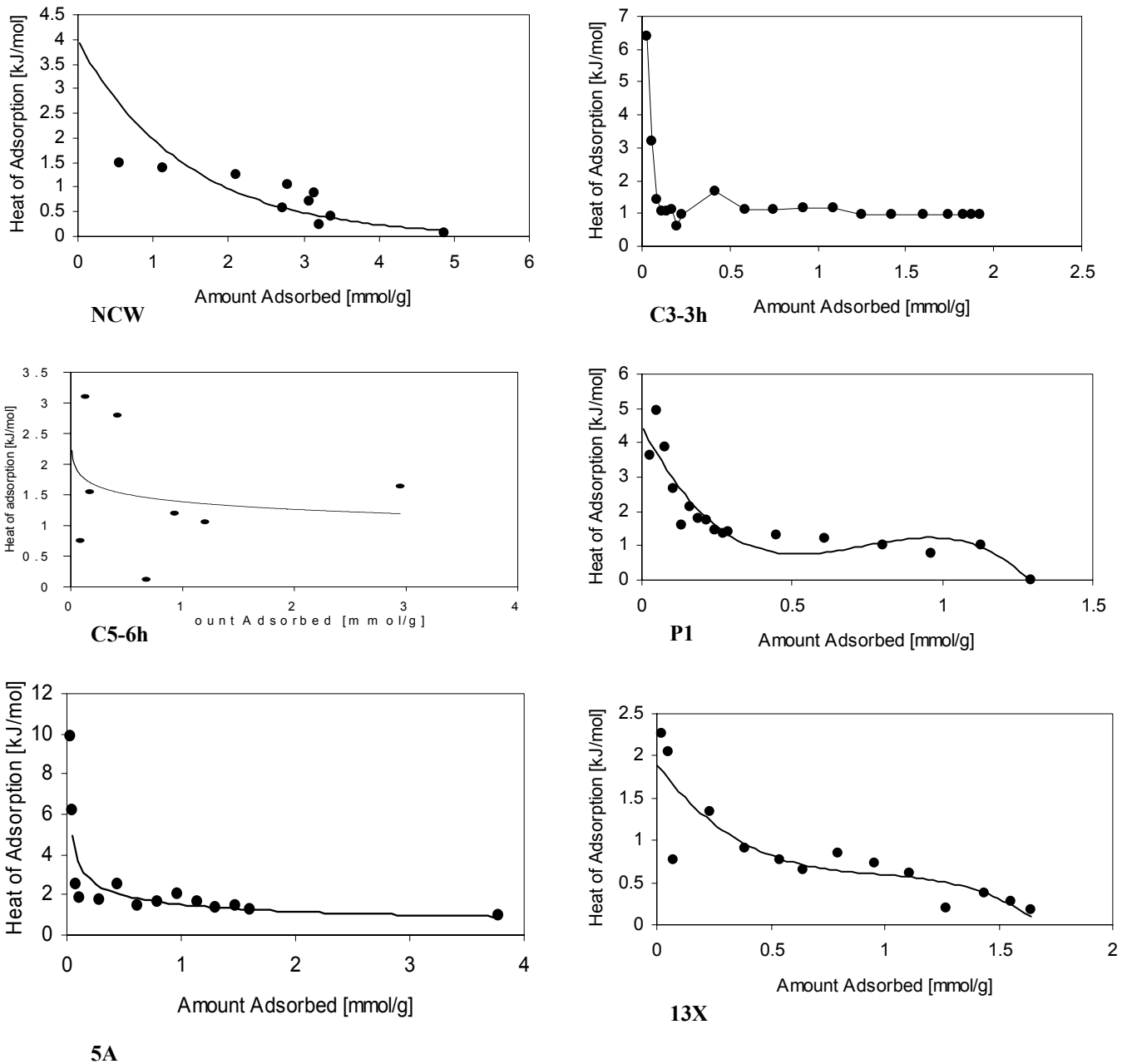


Figure 6.14: Differential Heat of Adsorption of Ar on Zeolites

As can be seen from Figure 6.14 the heat of adsorption values at zero coverage for all the zeolites are lower than for N₂ and CO₂. The main reason for that can be explained as Ar gas doesn't have a quadrupole moment and hence interaction of Ar with the zeolites is not specific for the Lewis or the Bronsted acidic sites, but involves only a nonspecific interaction dominated by dispersive forces. The highest zero coverage heat of adsorption belongs to 5A zeolite which also exhibits the highest interaction for CO₂.

Table 6.10: Comparison of the heat of adsorption values of the zeolites at zero coverage

Zeolites	Si/Al	Heat of ads at zero loading [kJ/mol]			Reference
		CO ₂	N ₂	Ar	
NCW	4.04	80.39	9.10	3.96	This study
NZ*			10.72		Ackley and Yang, 1991
C1-6h	5.25	38.54	1.83	-	This study
C3-3h	6.08	37.52	6.38	6.03	This study
C5-6h	8.4	55.99	3.92	1.39	This study
P1	5.01	79.5	8.86	4.40	This study
5A	0.98	83.08	7.31	9.86	This study
13X	1.35	72.75	5.20	1.90	This study
13X	1.23	49.1	19.9	12.7	Dunne et.al,1996

* Untreated natural zeolite

The heat of adsorption values of the zeolites under investigation at zero coverage are compared in Table 6.10. It can be concluded that in all the adsorbents, adsorption heats of CO₂ gas is the highest due to polarizabilities and the quadrupole moments of the CO₂ gas. For Ar gas it is the lowest since it's weakly adsorbed by the adsorbents. The highest adsorption heat value among the acid treated natural zeolites belongs to P1 zeolite for CO₂ which is due to its lowest Si/Al ratio. When taking into consideration the heat of adsorption values of CO₂ on the adsorbents, the heat of adsorption values in decreasing order are approximately; 5A > P1 > ~ NCW > 13X > C5 > C1 which are approximately consistent with the results obtained from adsorption studies. The reason for having similar adsorption heats for P1 and NCW is due to the proximity in their Si/Al ratios which are 5.01 and 4.04 for P1 and NCW respectively. Naturally the heat of adsorption values should decrease in the order of increasing Si/Al ratio since, according to the degree of dealumination, the surface of

the adsorbent becomes more homogeneous due to the reduction of the specific interactions between the adsorbent surface and the adsorbate gas. However, heat of adsorption value of zeolite C5-6h is greater than that of C1-6h and C3-3h. The reason for this can be explained in such a way that although the specific interactions are reduced as the degree of dealumination increases, the acidic strength of the strong Bronsted sites increases with the dealumination level (Aurox A., 2002) ;hence producing more active sites. Therefore, the heat of adsorption of C5-6h zeolite is greater than that of C1-6h and C3-3h zeolites. Another important parameter to be considered is the cation size in which the gas molecules interact with during adsorption. In fact, interactions decrease with increasing cation size (Savitz et al., 2000). Aurox (1997) reported that, zeolites with large pores display lower adsorption heats than medium or small pore size zeolites. Their number of acid sites per unit cell is also lower. Therefore, gas molecules may interact with smaller exchangeable cations of the adsorbent; hence, exhibiting lower adsorption heat values. When the pore diameters of the zeolites are investigated (Table 5.3), it is seen that P1 zeolite with smaller pore diameters has higher heat of adsorption observed for P1 zeolite while in C5-6h zeolite with an apparent median pore diameter of 6.3 Å, lower heat of adsorption value is determined. This indicates that as pore size increases, heat of adsorption value decreases.

On the other hand, 5A synthetic zeolite which is untreated has the highest heat of adsorption value which may be due to the Si/Al ratio that it possesses. Also, the interactions with the probe molecules are specific and very strong.

Washed natural zeolite (NCW) has a high heat of adsorption value because natural zeolites are usually heterogeneous materials when not treated with any method.

When Table 6.10 is investigated, it can be said that in most of the adsorbents, CO₂ gas has the highest heat of adsorption value at zero coverage while Ar has the lowest due to properties of the gas molecules.

6.3. Determination of the Isosteric heat of Adsorption

The isosteric heat of adsorption of a gas is a key variable for the design of adsorptive gas separation processes. For pure gas adsorption the heat is defined by;

$$q^{\circ} = -[\delta H^{\circ}/\delta n^m]_T \quad (6.4)$$

where q° is the isosteric heat of adsorption of a pure gas at an adsorbate loading of n^m and temperature T . H° is the specific enthalpy and n^m is the specific amount adsorbed (Siperstein et al., 2000). The corresponding gas-phase pressure is P .

The definition of q° given by above equation has recently been used to design calorimetric experiments for the direct measurement of isosteric heats as a function of n^m at constant T (Cao et al., 2001).

The above equation is equivalent to:

$$q^{\circ} = -R [\delta \ln P / \delta (1/T)]_{n^m} \quad (6.5)$$

Plots of $\ln P$ as a function of reciprocal absolute temperature at constant loading are called adsorption isosteres.

The isosteric heat of adsorption of CO_2 and N_2 on the zeolite samples are determined by constructing the plots of $\ln (P)$ vs $\ln 1/T$.

Table 6.11. Heat of Adsorption values of CO₂ and N₂ on the zeolites

	CO ₂				N ₂			
<i>C1-6h</i>								
n [mmol/g]	-	-	-	-	0.028	0.03	0.054	0.076
q ^o [kJ/mol]	-	-	-	-	55.4	54.2	35.7	48.7
<i>C3-3h</i>								
n [mmol/g]	0.35	0.87	1.5	1.65	0.1	0.16	0.21	0.23
q ^o [kJ/mol]	10.6	12	14	14	12.2	14.2	17.8	19
<i>C5-6h</i>								
n [mmol/g]	0.13	0.87	1	1.4	0.07	0.09	0.11	0.16
q ^o [kJ/mol]	9.7	7.5	3.5	3.6	8.7	9.1	8.4	11.1
<i>5A</i>								
n [mmol/g]	0.14	0.82	2.35	5.47	0.02	0.08	0.17	0.58
q ^o [kJ/mol]	30.2	34.5	32.3	0.004	19.1	27.3	27.2	27.9
<i>PI</i>								
n [mmol/g]	1.64	1.74	1.83	1.92	0.14	0.24	0.29	0.31
q ^o [kJ/mol]	69.88	60.86	55.21	47	20	19.2	18.9	20.8
<i>N2</i>								
n [mmol/g]	-	-	-	-	0.07	0.13	0.15	0.18
q ^o [kJ/mol]	-	-	-	-	13.1	16.2	16.5	18.6
<i>NCW</i>								
n [mmol/g]	1.64	1.83	1.93	2.04	0.22	0.35	0.42	0.5
q ^o [kJ/mol]	31.1	23.1	23.03	14	2.87	3.45	4.17	4.39

Table 6.11 presents the heat of adsorption values calculated theoretically at different n values for CO₂ and N₂ adsorption. Table 6.11 shows that for N₂ adsorption, isosteric heats calculated theoretically by Clasius-Clapeyron equation are fluctuated with increasing n values for C1-6h and C5-6h zeolites which indicate that these adsorbents are comparatively homogeneous. Because, isosteric heat of adsorption is independent of n for an energetically homogeneous adsorbent. On the other hand, at increasing n values, isosteric heats of C3, N2 and 5A samples for N₂ adsorption increase which shows that the lateral interactions between the adsorbed molecules are strong. However, for CO₂ adsorption, as n increases isosteric heat

decreases which indicates that 5A zeolite is energetically heterogeneous for CO₂ adsorption. The same trend is also valid for C5-6h sample and it shows heterogeneity for CO₂. Besides for CO₂ adsorption, there is a decreasing trend in isosteric heats as adsorbate loading increases, which shows that samples are strongly heterogeneous and this was also supported by the interaction parameters of the Langmuir and Sips Models.

The adsorption capacities of the zeolites for N₂ are by a great extent consistent with the microcalorimetric data. Because, 5A and P1 samples have the highest adsorption capacities and they have fairly high heat of adsorption which are 7.31 and 8.86 kJ/mole respectively while C1 has the lowest heat of adsorption value of 1.83 kJ/mole and thus supports the result that C1 has the lowest adsorption capacity. As the specific interactions between the adsorbent and N₂ gas are increased, the gas molecules are more adsorbed by the adsorbents therefore as the heat of adsorption increased the adsorbed amount of the gas molecules increased.

Besides, the monolayer adsorption capacities for N₂ determined by Langmuir and Sips Models are consistent with the experimental data. The highest monolayer capacity calculated by these models at both temperatures belongs to 5A zeolite and the lowest one to C1 sample which is also consistent with the experimental results in microcalorimetry.

As a result, the comparison of the experimental results and theoretical results yield that for N₂, P1 zeolite has the highest heterogeneity among the acid treated natural zeolites. Besides, 5A zeolite has the highest heterogeneity for CO₂ due to the specific interactions. C5-6h and C1-6h zeolites are comparatively homogeneous due to their higher Si/Al ratio. However, the heat of adsorption values calculated theoretically for CO₂ are lower than the values obtained experimentally. Auroux states that (1997), in the case of zeolitic systems, the values of adsorption heats obtained experimentally and theoretically differ quite considerably. Differences can be attributed to the fact that in calculating isosteric heats of adsorption using the Clasius-Clapeyron equation, it is difficult to evaluate accurately a derivative from an experimental curve. Direct calorimetric measurements are free from such deviations and provide more reliable data.

CONCLUSION

Clinoptilolite-rich natural zeolitic tuff from Gördes, Findıcak region (Manisa, Turkey) treated with HCl, HNO₃ and 1.1 M H₃PO₄ acid solutions and synthetic zeolites namely 5A and 13X have been investigated through volumetric and calorimetric studies by using adsorption of CO₂, N₂ and Ar gases. In volumetric studies, the adsorption isotherms of these gases on the zeolites were obtained at 5°C and 25 °C. Model equations such as Langmuir, Sips, Dubinin Astakhov were applied to the adsorption data in order to get information regarding the heterogeneity of the acid treated natural zeolites and the results were compared with the untreated natural zeolite and commercial synthetic zeolites. Besides, potential energy distributions of the adsorbent-adsorbate systems were analyzed because the heterogeneity of the microporous adsorbents is connected closely with the distribution of adsorption potential in micropores. These distributions characterize the energetic heterogeneity of microporous solids.

Adsorption studies showed that the amount adsorbed increased with decreasing adsorption temperature for both gases. Among the acid treated natural zeolites, the zeolites treated with 1.1 M H₃PO₄, P1 has the highest adsorption capacity (2.24 mmol/g and 0.67 mmol/g) for CO₂ and N₂ while the natural zeolites has only 2.08 mmol/g and 0.51 mmol/g respectively at 5°C. Synthetic zeolites 13X and 5A have higher CO₂ (6.82 mmol/g and 5.46 mmol/g respectively) and N₂ amount (0.31mmol/g and 0.91 mmol/g) adsorbed at 5 °C. In N₂ adsorption, Langmuir b parameter called the affinity constant decreased as adsorption temperature increased. Another model applied to the experimental data is the Sips adsorption model equation. The Sips model t parameter characterizing the system heterogeneity is higher for CO₂ adsorption than N₂ adsorption and decreases with increasing temperature. This indicates that the CO₂ molecules give the more specific interactions than N₂ molecule. The Langmuir equation was applied to the data for calculation of the Henry's constant. The pure component selectivity of CO₂ over N₂ are the highest for NCW zeolite and P1 sample follows it which are 408 and 151 at 25°C respectively. The selectivity is the highest when Si/Al ratio is around 4. Unlike Henry constants for N₂, Henry constants for CO₂ were determined to be effected significantly by the change of the Si/Al ratio due to strong specific interactions between the quadrupole moment of CO₂ and the adsorbents.

The results obtained calorimetrically were generally consistent with the adsorption data. According to this, P1 was determined to have the highest heat of adsorption at zero coverage among the acid treated natural zeolites (while washed natural zeolite (NCW) has a close adsorption heat with the P1 sample which were approximately 80.29 and 80.39 kJ/mole. Besides, 5A zeolite has the highest heat of adsorption at zero coverage which indicates that it's the most heterogeneous among the zeolites. These results are consistent with the ones obtained from adsorption studies. Finally, by using the Clasius-Clapeyron Equation isosteric heat of adsorption values for the zeolites were calculated theoretically in order to compare with the ones obtained from microcalorimetry experimentally. These results also indicated that 5A and P1 samples are heterogeneous. However, adsorption heats obtained experimentally are greater than the ones obtained theoretically. Differences can be attributed to the fact that in calculating isosteric heats of adsorption using the Clasius-Clapeyron equation, it is difficult to evaluate accurately a derivative from an experimental curve. Direct calorimetric measurements are free from such deviations and provide more reliable data.

REFERENCES

1. Ackley M.W., Giese R.F., Yang R.T., "Clinoptilolite: Untapped potential for kinetic gas separations," *Zeolites*, 12 (1992) 780-788
2. Ackley M.W., Yang R.T., "Adsorption characteristics of high-exchange clinoptilolites," *Ind. Eng. Chem. Res.*, 30 (1991) 2523-2530
3. Armenta G.A., Jimenez L.D., "Characterization of the porous structure of two naturally occurring materials through N₂-adsorption (77K) and gas chromatographic methods, *Colloid and Surfaces*, 176 (2001) 245-252
4. Armenta G.A., Ramirez G.H., Loyola E.F., Castaneda A.U., Gonzalez R.S., Munoz C.T., Lopez A.J., Castellon E.R., "Adsorption kinetics of CO₂, O₂, N₂ and CH₄ in cation-exchanged clinoptilolite," *J. Phys. Chem B*, 105 (2001) 1313-1319
5. Auroux A., "Acidity characterization by microcalorimetry and relationship with reactivity," *Topics in Catalysis*, 4 (1997) 71-89
6. Auroux A., "Microcalorimetry methods to study the acidity and reactivity of zeolites, pillared clays and mesoporous materials," *Topics in Catalysis*, 19 (2002) 205-213
7. Becer M., (2003), *Ms Thesis*, Izmir Institute of Technology, Turkey
8. Bolis V., Broyer M., Barbaglia A., Busco C., Foddanu G.M., Ugliengo P., "Van der Waals interactions on the acidic centres localized in zeolites nanocavities: a calorimetric and computer modeling study", *Journal of Molecular Catalysis A: Chemical*, 204-205 (2003) 561-569
9. Clarkson C.R., Bustin R.M., " Binary gas adsorption/desorption isotherms effect of moisture and coal composition upon carbon dioxide selectivity over methane," *International Journal of Coal Geology*, 42, (2000), 241-271
10. Çakıcıoğlu F., Ülkü S., "Adsorption characteristics of Lead-, Barium- and hydrogen rich clinoptilolite mineral", *Adsorption Science and Technology*, 21(2003), 309-317
11. Demirci A., (1996), *Ms Thesis*, Ege University, Turkey
12. Do D.D., Adsorption Analysis: Equilibria and Kinetics, (Imperial College Press, 1998)
13. Dunne J.A., Sircar S., Gorte R.J., Myers A.L., "Calorimetric heats of adsorption and adsorption isotherms.2. O₂, N₂, Ar, CO₂, CH₄, C₂H₆ and SF₆ on NaX, H-ZSM-5, and Na-ZSM-5," *Langmuir*, 12 (1996) 5896-5904

14. Gil A., Grange P., "Application of the Dubinin-Radushkevich and Dubinin-Astakhov Equations in the characterization of the microporous solids," *Colloids and Surfaces*, 113, (1996), 39-50
15. Guil J.M., Garcia J. E., Paniego A.R., Menayo J.M., "Gas/surface titration microcalorimetry. Energetics of oxygen adsorption on supported iridium catalysts," *Topics in catalysis*, 19 (2002) 313-321
16. Guil J.M., Melon J.A., Carvalho M.B., Carvalho M.B., Pires J., "Adsorption microcalorimetry of probe molecules of different size to characterize the microporosity of pillared clays," 51 (2002) 145-154
17. Huesca R.H., Diaz L., Armenta G.A., "Adsorption equilibria and kinetics of CO₂, CH₄ and N₂ in natural zeolites," *Separation Purification Technology*, 15 (1999) 163-173
18. Jayaraman A., Yang R.T., "Adsorption of nitrogen, oxygen and argon on Na-CeX zeolites," *Adsorption*, 8 (2002) 271-278
19. Karacan Ö.C., Okandan E., "Assessment of energetic heterogeneity of coals for gas adsorption and its effect on mixture predictions for coalbed methane studies," *Fuel*, 79 (2000) 1963-1974
20. Kluson P., Scaife S., Quirke N., "The design of microporous graphitic adsorbents for selective separation of gases," *Separation Purification Technology*, 20 (2000) 15-24
21. Mathias M.P. Kumar R., Moyer D.J., Schork M.J., Srinivasan S.R., Talu O., "Correlation of multicomponent gas adsorption by the dual-site Langmuir model. Application to nitrogen/oxygen adsorptions. on 5A zeolite," *Ind. Eng. Chem. Res* 35 (1996) 2477-2483
22. Pakseresth S., Kazemeini M., Akbarnejad M.M., "Equilibrium isotherms for CO, CO₂, CH₄ and C₂H₄ on the 5A molecular sieve by a simple volumetric apparatus," *Separation and Purification Technology*, 28 (2002) 53-60
23. Rakic V., Dondur V., Hercigonja V., "Thermal effects of the interactions of carbon monoxide with zeolites," *Thermochimica Acta*, 379 (2001) 77-84
24. Rakic V., Dondur V., Mioc U., Jovanovic D., "Microcalorimetry in the identification and characterization of the most reactive active sites of heterogeneous catalysts," *Topics in Catalysis*, 19 (2002) 241-247
25. Rege S.U., Yang R.T., Buzanowski M.A., "Sorbents for air prepurification in air separation," *Chemical Engineering Science*, 55 (2000) 4827-4838

26. Rozwadowski M., Wojsz R., Wisniewski K.E., Kornatowski J., "Description of adsorption equilibrium on type A zeolites with use of the Polanyi-Dubinin potential theory," *Zeolites*, 9 (1989) 503-508
27. Ruthven D.M., Principles of Adsorption Processes (John Wiley and Sons, 1984)
28. Sakuth M., Meyer J., Gmehling J., "Measurement and prediction of binary adsorption equilibria of vapors on dealuminated Y-zeolites (DAY)," *Chemical Engineering and Processing*, 37, (1998) 267-277
29. Savitz S., Myers A.L., Gorte R.J., "A calorimetric investigation of CO, N₂, and O₂ in alkali-exchanged MFI," *Microporous and Mesoporous Materials*, 37 (2000) 33-40
30. Rouquerol F., Rouquerol J., Sing K., Adsorption by powders and porous solids (Academic Press, 1999)
31. Sircar S., "Applications of Gas Separation by Adsorption for the Future," *Adsorption Science and Technology*, 2001
32. Sircar S., Rao M.B., "Effect of adsorbate size on adsorption of gas mixtures on homogeneous adsorbents," *AIChE Journal*, 45 (1999) 2657-2661
33. Solinas V., Ferino I., "Microcalorimetric characterisation of acid-basic catalysis," *Catalysis Today*, 41 (1998) 179-189
34. Talu O., Li J., Kumar R., Mathias M.P., Moyer D.J., Schork M.J., "Measurement and analysis of oxygen/nitrogen/5A-zeolite adsorption equilibria for air," *Gas Separation Purification*, 10, (1996), 149-159
35. Talu O., Zwiebel I., "Multicomponent adsorption equilibria of nonideal mixtures," *AIChE Journal*, 32 (1986) 1263-1276
36. Triebe R.W., Tezel F.H., "Adsorption of nitrogen and carbon monoxide on clinoptilolite: Determination and prediction of pure and binary isotherms," *The Canadian Journal of Chemical Engineering*, 73 (1995) 717-724
37. Ustinov E.A., "Multicomponent equilibrium adsorption on heterogeneous adsorbents," *Adsorption* 6 (2000) 195-204
38. Webster C.E., Drago R.S., "The multiple equilibrium analysis quantitative prediction of single and multi-component adsorption isotherms on carbonaceous and zeolitic solids," *Microporous and mesoporous materials*, 33 (1999) 291-306

APPENDIX

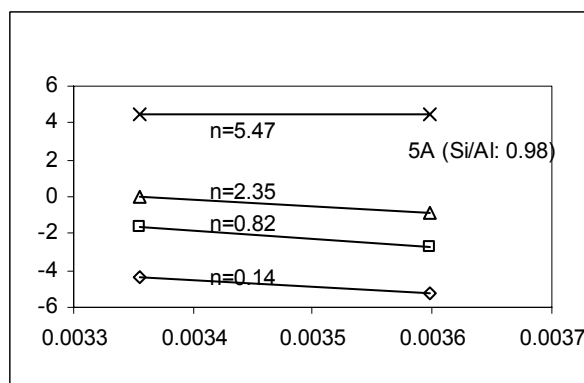
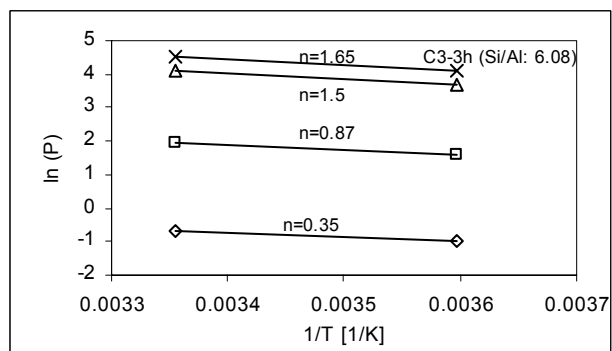
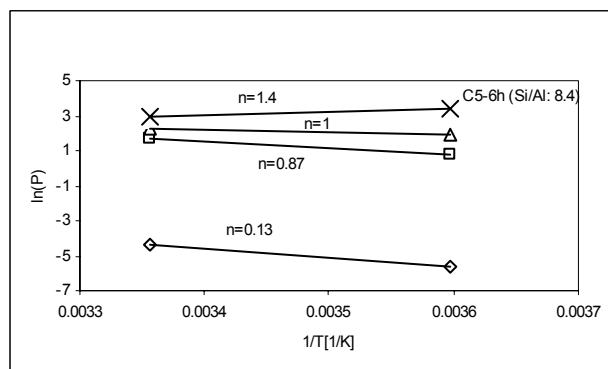
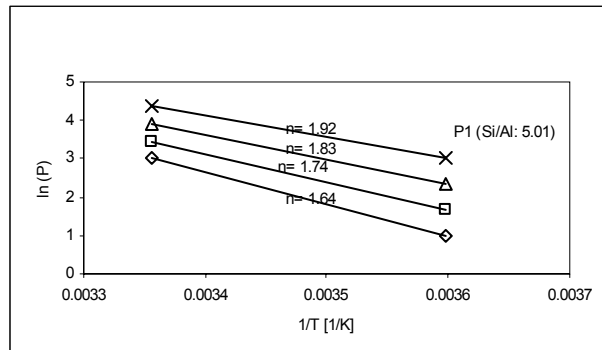
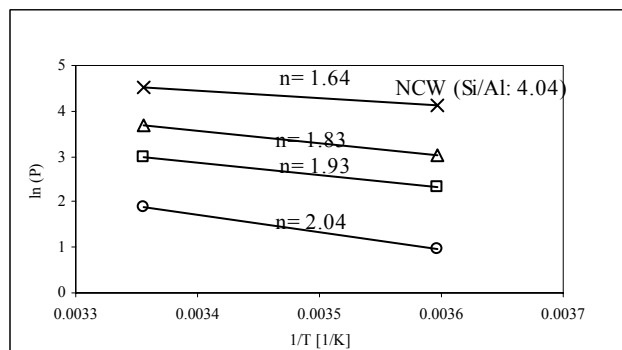


Figure 1: Isotheres for adsorption of CO₂ at 5 °C and 25 °C

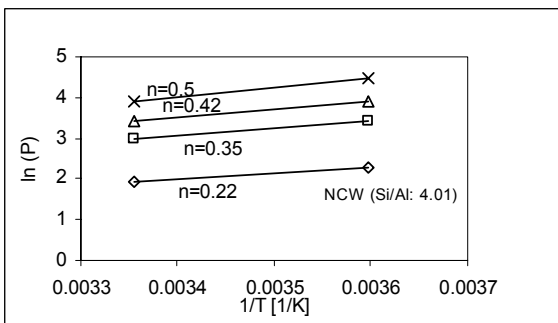
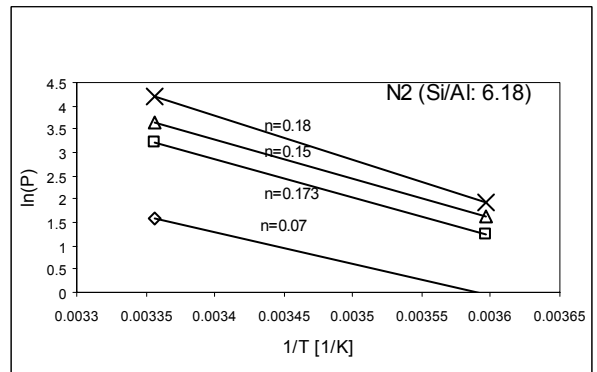
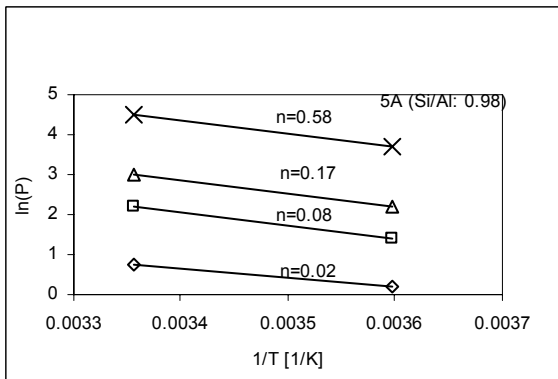
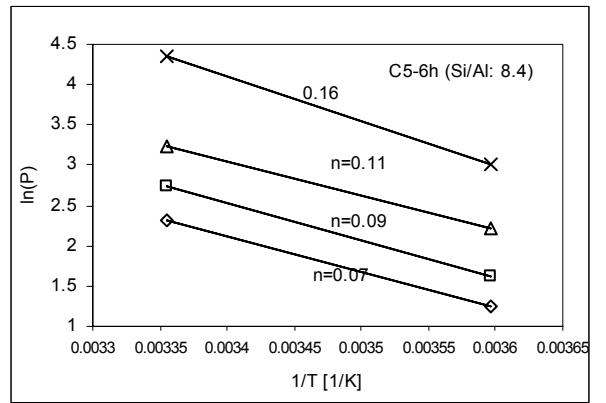
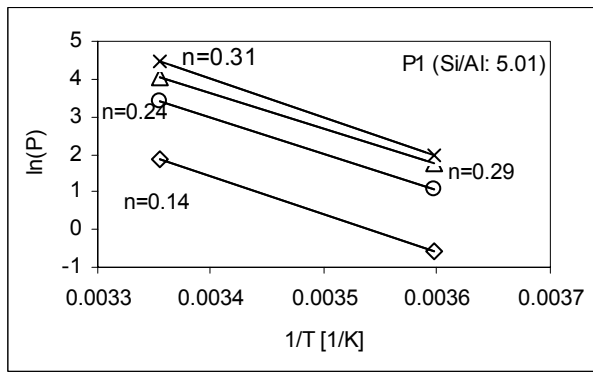
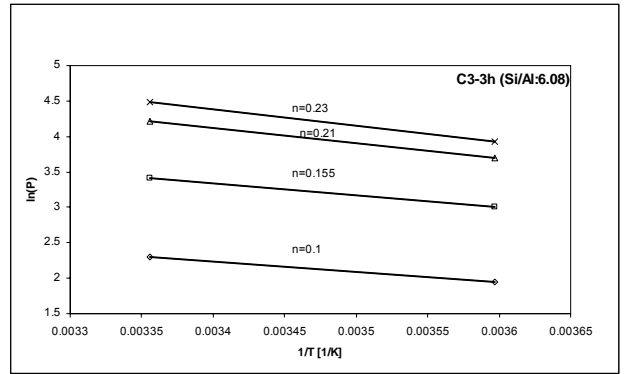
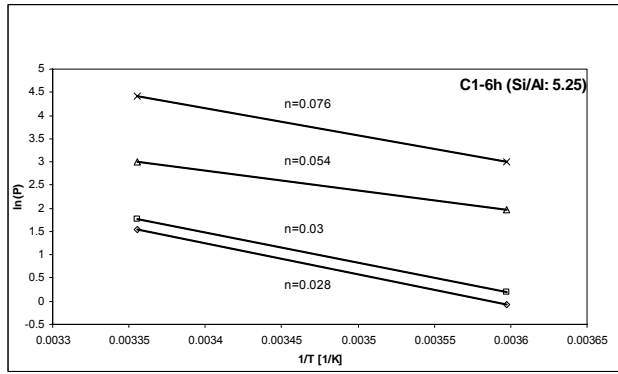


Figure 2: Isosteres for adsorption of N₂ at 5 °C and 25 °C